Applications and limitations of trace elements-accessory phase thermometry

Thesis submitted for partial fulfillment of M.Sc. Degree in Applied Geology,2019

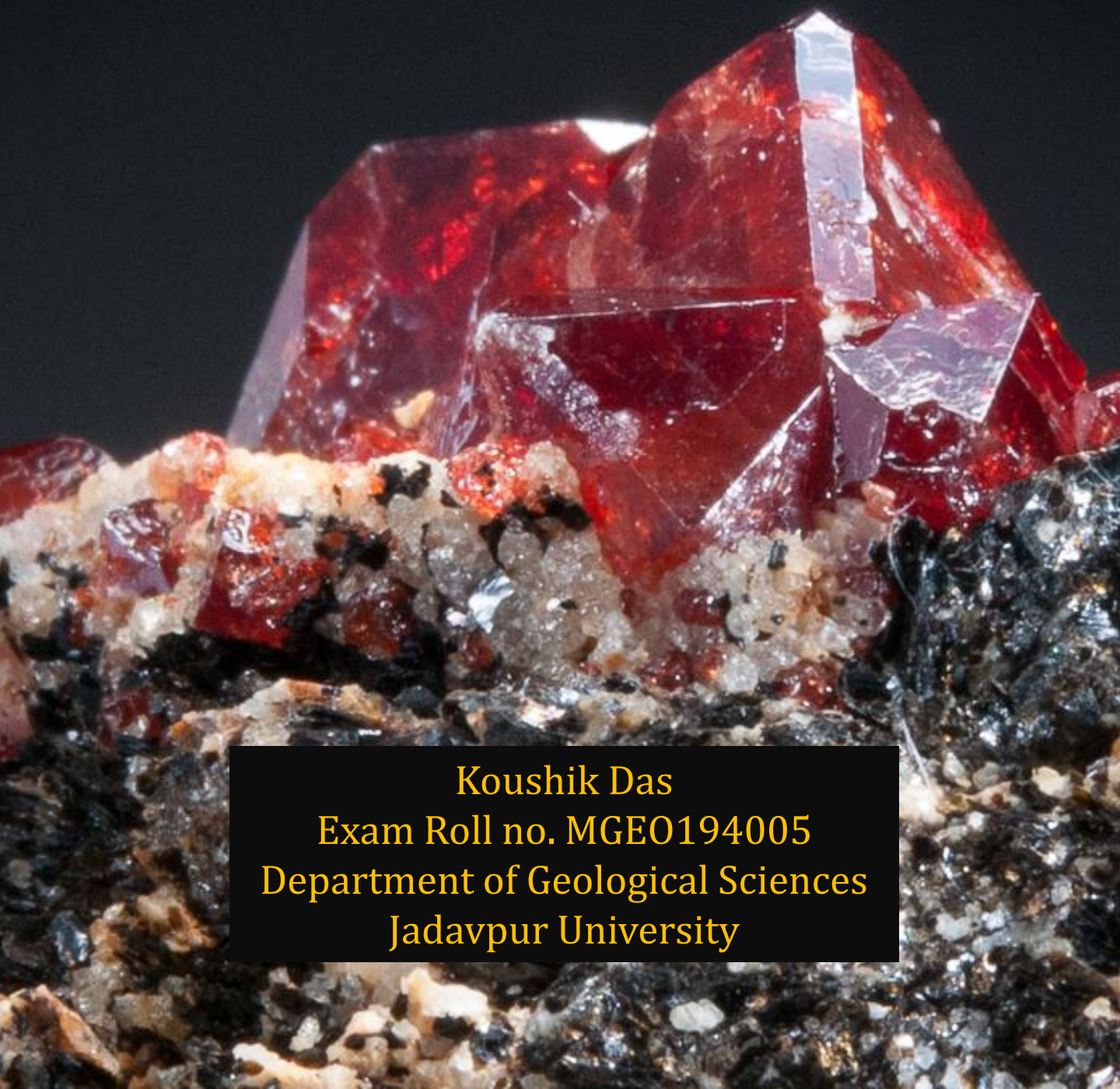

Koushik Das
Exam Roll no. MGEO194005
Department of Geological Sciences
Jadavpur University

Applications and limitations of trace elements-accessory phase thermometry

Thesis submitted for partial fulfillment of M.Sc. Degree in Applied Geology,2019

Koushik Das

Exam Roll no: MGEO194005

Class Roll no: 001720402004

Registration no: 128243 of 2014-15

Department of Geological Sciences

Jadavpur University

Under the guidance of

Prof. Pulak Sengupta

যাদবপুর বিশ্ববিদ্যালয়
কলকাতা-৭০০০৩২, ভারত

JADAVPUR UNIVERSITY
KOLKATA-700032, INDIA

FACULTY OF SCIENCE : DEPARTMENT OF GEOLOGICAL SCIENCES

CERTIFICATE FROM THE SUPERVISOR

This is to certify that **Mr. Koushik Das** has worked under the supervision of Prof. Pulak Sengupta in the Department of Geological Sciences, Jadavpur University and completed his thesis entitled **"Applications and limitations of trace elements-accessory phase thermometry"** which is being submitted towards the partial fulfillment of his M.Sc. Final Examination in Applied Geology of Jadavpur University in 2019.

Signature of the Supervisor:

Prof. Pulak Sengupta
Dept. of Geological Sciences
Jadavpur University

Dr. Pulak Sengupta
Professor
Department of Geological Sciences
Jadavpur University, Kolkata-700032

Signature of Head of the Department:

30/05/2019

Prof. Sanjoy Sanyal
Dept. of Geological Sciences
Jadavpur University

Head
Department of Geological Sciences
Jadavpur University
Kolkata-700032

দূরভাষ : ২৪১৪-৬৬৬৬/প্রসারণ : ২২৬৮
Website : www.jadavpur.edu
E-mail : hod_geological@jdvu.ac.in
Phone : 2414 6666/Extn. 2268

Contents

Abstract

The partition of Zr and Ti in the coexisting rutile and zircon is inferred to be a function of temperatures. The robustness of these two accessory phases, their common occurrence in a variety of magmatic and metamorphic rocks and sluggish diffusion of tetravalent elements (Ti^{4+} and Zr^{4+}) make these thermometers appropriate for constraining the temperatures of magmatic and metamorphic rocks. Ti-in-zircon thermometer is commonly considered as pressure-insensitive but experimental studies showed that Zr-in-rutile depends on pressure. The present study evaluates the applicability of these thermometers with the help of natural examples reported from different metamorphic rocks. The study reveals that for Zr-in-rutile thermometer, the calibration by Watson (2006, pressure insensitive) yield temperatures similar to calibrated by Tomkins (2007) for alpha and beta quartz fields up to the pressure of 12 kbar. However, at high pressure (>25kbar), the coesite field calibration of Tomkins(2007) yield higher temperature than the calibration of Watson (2006). The study also shows that in most of the cases the Zr-in-rutile thermometers yield higher temperatures than the temperatures recorded in Ti-in-zircon thermometry. Both the thermometers yield wide temperature ranges which deviates significantly from the results of the independent thermometer applied to corresponding rocks. The reasons for the variation include post-peak alteration and retrogression, diffusion, effective removal of one of the phases by getting included in porphyroblastic phases and lattice defect. The results are specifically ambiguous for high to ultra-high temperature metamorphic rocks. Therefore, this study emphasizes that the results of these trace element exchange thermometers should be coupled with other results of other independent geothermometers to record meaningful temperature estimates for magmatic and metamorphic rocks.

Introduction

Geothermometers represent mineral system that is used to estimate the temperatures at which metamorphic mineral assemblage equilibrates. Element partitioning in these minerals is a kind of chemical reaction which is often guided by the temperature (Ferry and Spear, 1978). These temperature estimates are valuable in constraining the peak conditions of metamorphism which is used to establish the P-T-t paths and probable tectonic scenarios. Fe-Mg exchange thermometers for different mineral pairs (viz. garnet-orthopyroxene, garnet-clinopyroxene, and garnet-biotite) have long been used to constrain the physical conditions of metamorphism. However, diffusion of Fe-Mg often hinders these estimates. In the last decade, the experimental and natural studies have shown that concentration of tetravalent trace elements in accessory phases (Ti-in-zircon and Zr-in-rutile) is sensitive to temperature and can be used as effective geothermometer to constrain the metamorphic (Zack et al. 2004; Watson et al. 2006; Ferry & Watson 2007) and magmatic temperature (Rubatto & Hermann 2007; Zhang et al. 2010). Experimental studies also showed that uncertainty of these two thermometers is estimated to be ± 10°C or better (Watson & Harrison 2005; Watson et al. 2006). The sluggish diffusion of these high valence elements (Ti, Zr) further provides appropriate constrains for metamorphic temperatures. Zircon and rutile are two common accessory phases that are found in a wide variety of magmatic and metamorphic rocks. These phases also control the trace element budget in the rock (Bea et al. 1992). These phases are also considered to be robust and less susceptible to post-peak retrogression or alterations (Cherniak and Watson, 2007). Henceforth, Ti-in-zircon thermometer is believed to be important particularly for constraining the peak temperatures of granulite-ultra high temperature metamorphic rocks. Rutile, on the other hand, occurs in different microstructural assemblages and hence, Zr-in-rutile helps to

pinpoint the temperatures of the mineral assemblages that become stable at different parts of a P-T path. Zircon often incorporates crucial radiogenic elements which makes it an efficient geochronometer. It helps to constrain the timing of magmatism and metamorphic pulses in polydeformed terranes (Harley 2007). Combination the date and temperatures recovered from zircon helps to evaluate detailed P-T-t evolution of metamorphic rocks.

Although Ti-in-zircon and Zr-in-rutile have provided reliable temperature estimates for variety of metamorphic rocks, there are significant number of studies that reports ambiguity between the temperatures estimated from accessory phase thermometers and that of the independent thermometers. The present study compares the results yielded by these two thermometers and aims to investigate the validity of these two thermometers with respect to variety of metamorphic rocks reported from different parts of the world covering a wide range of P-T conditions varying from amphibolite to ultra high temperature granulites and eclogites. The study also evaluates the effect of pressure on the thermometers.

Theory

Studies have shown that accessory phases contain substantial amount of REE and trace element s as functions of the structure of the accessory phases and ambient physicochemical conditions. In the following sections, structures, distributions in natural rocks and compositional variation (in terms of race elements) zircon and rutile are presented.

Zircon

Zircon (Zr[SiO4]) is one of the common mineral that occur in variety of rocks covering a wide range of composition and mineral assemblages.The name derives from the Persian *zargun*, meaning "gold-hued". This word is corrupted into "jargoon", a term applied to light-colored zircons. The English word "zircon" is derived from *Zirkon*, which is the German adaptation of this word.It is an orthosilicate, in the zircon structure each silicon atom is surrounded by a tetrahedral group of four oxygen atoms at a distance of 1.61 Å, while each zirconium atom lies between four oxygen atoms at 2.15 Å and four at a distance of 2.29 Å. One of the major importance of zircon is that it takes two of the most abundant radiogenic elements i.e. U and Th and does not take non-radiogenic Pb in its structure (Watson and Harrison, 1984; Watson et al.2006; Harley 2007) which makes it an effective geochronometer. Zircons crystallize in terrestrial environments ranging from the high pressure–temperature conditions of the upper mantle (e.g., Davis et al. 1976) to near-surface hydrothermal systems (e.g., Kerrich and King 1993). They have also been found in lunar rocks and in meteorites. Owing to its robustness, zircon remains stable over a range of pressure temperature conditions and often withstands tectonothermal events (Harley 2007). Zircon remain stable even under extreme high grade metamorphism , during which it may develop overgrowth

on preexisting magmatic or detrital crystals of zircons. and therefore, can be used to constrain the timing of metamorphism from polymetamorphosed terrane. Zircon often contains considerable amount of other radiogenic isotopes (Lu, Hf) which are often useful in monitoring the crustal growth, source composition and crust-mantle interactions (Vervoort, 2015).

Occurrence over a wide range of P-T conditions, physical and chemical durability, significant abundance of certain elements and resistance to diffusion makes zircon a useful geothermometer (Watson, 2006). Combining the results of high pressure temperature experiments and the natural examples it has been proposed that uptake of certain elements (i.e. Ti) is dependent on temperature (Watson, 2006, REF).

These features could be calibrated for use as a thermometer

Rutile

The name "rutile" is derived from the Latin word '*rutilus*' because of the deep red colour observed in some specimens in transmitted light. Rutile (TiO2) can be translucent or opaque. Yellowish and brownish colours are also very common (Guido Meinhold, 2010). Rutile has a density of 4.23 g cm^{-3}, but can range up to 5.50 g cm^{-3} (Deer et al., 1992), and thus belongs to the heavy mineral suite, which are minerals with density N2.8 g cm^{-3}. Rutile is commonly diamagnetic (non-magnetic), and therefore, it can easily be separated from the paramagnetic (weakly magnetic) and ferromagnetic (strongly magnetic) heavy mineral fraction using the Frantz isodynamic separator (Buist, 1963a). In nature, titanium dioxide mainly occurs in three structural states: rutile, anatase and brookite. Together they form the TiO2 end-member of the ternary system FeO–Fe2O3–TiO2. In the unit cell, each Ti4+ ion is surrounded by six oxygens at the corners of a slightly distorted, regular octahedron while each oxygen surrounded by three Ti4+ ions is lying in a plane at the

corners of an approximately equilateral triangle (Deer et al., 1992; Baur, 2007). Rutile is a high-pressure and high-temperature polymorph, The low-temperature polymorphs of titanium dioxide are anatase (tetragonal) and brookite (orthorhombic), Most naturally occurring rutile corresponds to the general formula TiO2, with titanium occurring as Ti4+.(Guido Meinhold,2010). Rutile breakdown occurs at the beginning of the greenschist facies and is newly formed at upper amphibolite facies conditions. Increasing pressure generally favours the formation of rutile, so that it is widespread at blueschist and eclogite facies conditionsin zircon-buffered assemblages, Zr incorporation in rutile appears to be temperature dependent. (Zack et al.2004).

Rutile in metamorphic rocks

Rutile is mainly formed during medium- to high-grade metamorphic processes (e.g. Goldsmith and Force, 1978; Force, 1980, 1991), but it can also form in low-grade metamorphic rocks (e.g Banfield and Veblen, 1991; Luvizotto et al., 2009a). Rutile in low- to medium-grade metamorphic rocks typically occurs as small (~20 – 100 μm), scattered grains, generally needle-like crystals, or polycrystalline aggregates. Rutile in high-grade and ultrahigh-grade metamorphic rocks (e.g. eclogites, granulites) forms mainly single crystals in the matrix but also occurs as inclusion in other minerals such as garnet, pyroxene, amphibole and zircon

Rutile in igneous rocks and mineralization

Additional sources of rutile can be quartz veins,granites,pegmatites, carbonatites, kimberlites and xenoliths of metasomatised peridotite and metallic ore deposits

Rutile in sedimentary rock

The largest sedimentary sources of rutile are fine-grained clastic sediment and heavy mineral sands (placer deposits). In sedimentary rocks rutile, anatase and brookite can form diagenetically from

Ti-rich pore-solutions, which may derive from alteration of ilmenite, titanite and biotite (Mader, 1980; Morad, 1986;Valentine and Commeau, 1990). Paine et al. (2005) ascribed alteration of ilmenite to pseudorutile and anatase in Pliocene placer deposits of southeastern Australia to postdepositional weathering.

Why use Accessory phase thermometers

In investigating high grade rocks particularly those formed at extreme metamorphic condition (T>900^{o}C) ,low closure temperature (<800oC) of the conventional geothermometers become susceptible to lower temperature resetting. An accurate estimate of peak temperature for high-grade rocks is often hampered by the significant re-equilibration or recrystallization during retrogression and cooling. This led to the recent development of trace element thermometers such as those based on titanium concentration in zircon and zirconium concentration in rutile (Liu et al. 2015).

Theoretical basis of the Thermometers

Ti in Zircon thermometer

The valence state of Ti is +4 and it does not change under any geological conditions (Watson 2006). Henceforth, Ti+4 enters into zircon structure replacing either Zr+4 through homovalent substitution involving any charge imbalance. Experiments of Ferry and Watson (2007) and the results of Harrison et al. (2005) suggest that the substitution occurs as :

$TiO_2 + ZrSiO_4 = ZrTiO_4 + SiO_2$

Watson and Harrison (2005) and Watson et al. (2006) experimentally determined that the Titanium content of zircon depends strongly upon temperature, varying by more than three orders of

magnitude over the ~850° temperature range investigated, and is relatively immune to changes in pressure. For a TiO2 staurated system, where rutile is present, the thermodynamic equation of the thermometer can be written as TiO2(rt)= TiO2(Zrn)

Following the equation mentioned above thermodynamic basis of Ti in Zircon thermometer is the reaction

The equilibrium constant is $k_1 = \frac{a_{TiO_2}^{zircon}}{a_{TiO_2}^{rutile}}$

where *a*TiO2 is the activity of TiO2 in rutile or zircon as indicated by the superscript. Because rutile is nearly pure TiO_2 so $a_{TiO_2}^{rutile} \sim 1$, so $k \cong a_{TiO_2}^{zircon}$

Therefore we get $a_{TiO_2}^{zircon} = \gamma_{TiO_2}^{zircon} X_{TiO_2}^{zircon} = \exp\left[\frac{-\Delta G_1^o}{RT}\right]$

γ is the activity coefficient

X is the mole fraction of TiO_2 in Zircon,

ΔG is the free energy change for the reaction when ‘‘reactant’’ and ‘‘product’’ are in their standard states,R is gas constant,T is absolute temperature,

Finally the following relationship between Ti concentration in zircon (in ppm by weight) and temperature: $T(^\circ\mathrm{C})_{zircon} = \frac{5080 \pm 30}{(6.01 \pm 0.03) - \log(\mathrm{Ti})} - 273$

The results of the thermometer have been extensively calibrated using both natural and synthetic samples which provided precision within ± 5°C.

This relation holds true if the zircon crystallizes in the presence of rutile and although the thermometer has been rigorously calibrated for rutile saturated conditions only, the thermometer is used widely for two reasons: first, because TiO2 activity in crustal rocks is generally high; and, second, because Ti is also taken up in quartz, so our Ti-in-zircon calibration can be used in conjunction with that of Wark and Watson (2004) for Ti in quartz to eliminate the dependence upon rutile (Watson et al. 2006).

Zr in Rutile Thermometry

Zr in rutile has been considered as a potential thermometer as the solubility of ZrO2 in rutile strongly depends on temperature and henceforth can be used when the rutile coexists with zircon + quartz (Zacket al., 2004; Watsonet al., 2006; Ferry& Watson, 2007). From the stand point of potential usefulness in thermometry, rutile actually has one advantage over zircon: rutile crystals usually grow in the presence of zircon (commonly accompanied by quartz), which means that in many cases the chemical potential of ZrO2 in the system is essentially fixed. It is thus possible that most or all variations in Zr content of natural rutile crystals are attributable to differences in temperature (or possibly pressure) (Watson et al.2006)

In zircon-buffered assemblages, Zr incorporation in rutile appears to be temperature dependent (Zack et al.2004). The dominant substitution taking place is $Zr^{4+} = Ti^{4+}$

At equilibrium, the relevant exchange reaction is $\mathrm{ZrO}_{2(\mathrm{zircon})} = \mathrm{ZrO}_{2(\mathrm{rutile})}$

The equilibirium constant is $k_2 = \dfrac{a_{\mathrm{ZrO_2}}^{\mathrm{rutile}}}{a_{\mathrm{ZrO_2}}^{\mathrm{zircon}}}$

If $a_{\mathrm{ZrO_2}}^{\mathrm{zircon}} = c$ (a constant), then $k_2 \cong a_{\mathrm{ZrO_2}}^{\mathrm{rutile}}/c$

So we have $a_{\mathrm{ZrO_2}}^{\mathrm{rutile}} = \gamma_{\mathrm{ZrO_2}}^{\mathrm{rutile}} X_{\mathrm{ZrO_2}}^{\mathrm{rutile}} = c \ \exp\left[\dfrac{-\Delta G_2^{\mathrm{o}}}{RT}\right]$

Finally the following relationship between Zr concentration in rutile(in ppm by weight) and temperature : $T\ (^{\circ}\mathrm{C})_{\mathrm{rutile}} = \dfrac{4470 \pm 120}{(7.36 \pm 0.10) - \log(\mathrm{Zr})} - 273$

However it was found that pressure plays a role because of the size difference between Zr^{4+}(0.72 Å) and Ti^{4+}(0.61 Å),as the rutile structure gets compressed in higher pressure the larger Zr^{4+} cation

will be less able to substitute Ti. So there is a pressure dependence, To investigate the pressure dependence of the thermometer, piston cylinder (at 10, 20 & 30 kbar) and 1 atm furnace experiments were performed in the system ZrO2-TiO2-SiO2 by Tomkins et al. in 2007. The solubility of ZrO2 in rutile, in the presence of zircon and quartz was reversed at each pressure value, they calibrated three temperature equations for different pressure fields

For Alpha Quartz field $$T(^{\circ}\mathrm{C}) = \frac{83.9 + 0.410P}{0.1428 - \mathrm{R}\ln\phi} - 273$$

For Beta Quartz Field $$T(^{\circ}\mathrm{C}) = \frac{85.7 + 0.473P}{0.1453 - \mathrm{R}\ln\phi} - 273$$

For Coesite Field $$T(^{\circ}\mathrm{C}) = \frac{88.1 + 0.206P}{0.1412 - \mathrm{R}\ln\phi} - 273$$

ϕ=Zr(ppm), P is in kbar, R is the gas constant, 0.0083144 kJ K^{-1}

Description of Samples

For application of Ti-in-zircon and Zr-in-rutile has been collected from different lithotypes. Details of the rocktypes, their metamorphic grades and sources have been listed in the Table 1.

The samples of Mitchell et al. (2018) and Korhonen et al. (2014) represent the Ultra high temperature metamorphosed rocks and were collected from the Eastern Ghats Province (EGP) of the Eastern Ghats Mobile Belt. The Eastern Ghats Mobile Belt is a polymetamorphic terrane located in the eastern part of the Indian peninsula. Discrete crustal blocks (terranes) bounded by large-scale shear zone systems have previously been identified based on the isotopic, metamorphic and lithological characteristics of the rocks. One such domain, the Eastern Ghats Province lies between the Godaravi rift to the south, the Kerajang shear zone to the north and the Sileru shear zone system to the west, many localities within the EGP province has evidence of UHT metamorphism. The EGP samples analysed by Mitchell et al. (2018) are garnet–cordierite–sillimanite granulites from Vizianagaram, The peak is constrained to >950 ^{o}C and 8 kbar by phase equilibirium studies. The Mg-Al granulites at Ananthagiri also yielded metamorphic peak temperature exceeding 1000 ^{o}C

The samples of Ewing et al. (2013) belong to the Ivrea-Verbano Zone (IVZ) in northern Italy. The IVZ comprises of two units: the Kinzigite Formation and the Mafic Complex. The Kinzigite formation comprises of amphibolite to granulite facies rocks comprising metapelites, metabasites, impure calcite marble and calc silicates. The mafic complex is an intrusive complex which is 10 km thick dominated by gabbro, norite, diorite which intruded or underplated the lower

crustal rocks of the Kinzigite formation. The metamorphic grade in the Kinzigite formation increases from amphibolite facies in the south to granulite facies in northwest. Granulite facies metamorphism was associated with widespread anatexis, producing strongly restitic metapelites with a high percentage of garnet and depleted trace element geochemistry indicating loss of 20–40 % granitic melt (Schnetger 1994). Rutile formed at the expense of high-Ti biotite as part of the melt-forming reaction (Schnetger 1994) in the highest-grade granulite facies metapelites (Zinggn1980; Luvizotto and Zack 2009). The high temperature of metamorphism by phase equilibrium modeling has been found to be 3.5–6.5 kbar and 650–730 ^{o}C in the amphibolite facies, to 10–12 kbar and 900–950 ^{o}C in the granulite facies. All samples collected are granulite facies metapelites, targeted as the only lithology in the IVZ that contains abundant large rutile.

The samples of Qiao et al. (2016) were reported from the Qianlishan-Helanshan Complex of the Khondalite Belt, western block of the North China Craton, The Qianlishan-Helanshan Complex is located in the westernmost part in the Khondalite Belt. They contain similar rock assemblages, mainly including Al-rich gneiss/granulite, quartzite, marble and calc-silicate rocks, collectively called the 'khondalites'. Recently, high-pressure pelitic granulites have been discovered in the Qianlishan-Helanshan Complex (Zhou et al., 2010; Yin et al., 2014, 2015).The pelitic granulites were subjected to four stages of metamorphism, the early prograde (M1), peak high-pressure (M2), post-peak decompression (M3) and late retrograde (M4) stages. The P-T conditions of early prograde assemblage (M1) are 9.3–9.7 kbar/656–674◦C, P-T conditions of the peak high pressure assemblage (M2) are 850–870◦C and 14–15 kbar. The post-peak decompressional stage (M3) is represented by formation of cordierite coronas at 4.5–5.0 kbar/780–785◦C, The late retrograde stage (M4) indicated by the formation of staurolite + chlorite in the matrix at 3.4–4.4 kbar/580–610 ◦C

The samples of Lin et al. (2018) belong to the North Qilian and Western Tianshan, China. The North Qilian NW-trending belt represent an early Paleozoic oceanic suture zone, a typical LT/HP metamorphic belt, that lies between the Alashan Block to the north and the Qilian Block to the south (Song et al.2009). In North Quilian samples were collected from Xiangzigou (QS45) and Baijingsi (2Q27 and 15BJS), about 40 km west and 30 km east of Qilian town, QS45 is a lawsonite–eclogite with a coarse-grained granular texture, 2Q27 is a lawsonite–eclogite, 15BJS is an epidote–eclogite, All three samples have been overprinted by blueschist-facies retrogression, The metamorphic PT conditions were found to be 2.2–2.6 GPa and 460–510°C. In western Tianshan the eclogite sample (HB121) was collected from the Habutengsu–Kebuerte eclogite facies unit in the UHP metamorphic zone, Eclogites in this unit occur as lenses of various sizes within massive garnet–phengite schists, Metamorphic PT conditions of 2.4–2.7 GPa, 550–570°C were found from phase equilibrium modeling and pseudosection studies.

The samples of Liu et al. (2015) represent Ultrahigh-pressure (UHP) eclogites from the northern Dabie orogen, central China. The Dabie orogen is located in the intermediate segment of the Qinling–Dabie–Sulu orogenic belt formed by the Triassic continental collision between the North China Block and South China Block (e.g., Xu et al., 1992; Li et al., 1993, 2000; Ames et al., 1996). It comprises several fault-bounded terranes with varying metamorphic grades, it is subdivided into five lithotectonic units from north to south (1) the Beihuaiyang zone (BZ); (2) the North Dabie complex zone (NDZ); (3) the Central Dabie UHP metamorphic zone (CDZ); (4) the South Dabie low-temperature (LT) eclogite zone (SDZ); and (5) the Susong complex zone (SZ).The lithotectonic units are separated by the Xiaotian–Mozitan fault, Wuhe–Shuihou fault, Hualiangting–Mituo fault and Taihu–Shanlong fault, respectively.

In addition to the high to ultra-high temperature rocks, a variety of UHP metamorphic rocks, including eclogite, gneiss, quartz, jadeitite, schist and impure marbles are also included (from CDZ and SDZ(South Dabie low-temperature (LT) eclogite zone), The occurrence of diamond and coesite in the metamorphic rocks from the CDZ indicates that the UHP metamorphism occurred at 700−850 °C and 2.8 GPa, the peak PT conditions of the eclogites in the SDZ were found 670 °C and 3.3 GPa. NDZ consists of tonalitic and granitic orthogneisses and post-collisional Cretaceous intrusions with metaperidotite, garnet pyroxenite, garnet-bearing amphibolite, granulite and eclogite, oriented mineral exsolutions in garnet and clinopyroxene,and the occurrence of micro-diamond in NDG banded gneisses indicates UHP and P>3.5GPa, NDZ eclogites experienced granulite-facies overprinting and later amphibolite-facies retrogression.

The samples of Spear et al. (2006) represent blueschist to eclogite facies rocks in the northern part of the island of Sifnos, Cyclades, Greece. Sifnos comprises of two lithotectonic facies, a northern predominantly blueschist and marble belt and a southeastern belt of predominantly greenschist facies overprinted by blueschists, the greenschist and blueschist are separated by a sharp boundary which resulted from fluid flow upward to the main marble unit.

The blueschists and eclogites of northern Sifnos are isoclinally folded and extensively sheared and flattened. Four generations of deformation have been recognized in terms of fabric and porphyroblasts relations in rocks from Sifnos (Lister and Raouzaios 1996).Samples were collected from nine localities comprising both metapelites and metabasites. The metapelites contain various proportions of garnet, phengite, paragonite, glaucophane, and quartz, with some samples containing epidote, chloritoid, and or jadeite, All samples of metapelite contain rutile and zircon both in the matrix and within garnet. Metabasites are comprised of garnet + omphacite + glaucophane ± epidote + paragonite ± phengite ± quartz ± ankerite + sphene + zircon. Rutile

typically occurs only as inclusions within garnet whereas sphene is present in the matrix of the metabasites. Sifnos blueschist–eclogite terrain has experienced a clockwise P–T path with maximum P–T conditions of 12–18 kbar and ca. 475°C

The samples of Chen et al. (2013) are from eclogites and veins from southwestern Tianshan, China. The blueschist–eclogite belt of southwestern Tianshan is located between the Yili–Central Tianshan and Tarim plates along the South Central Tianshan suture, mainly in Zhaosu county of Xinjiang province, China. It is bounded by two ductile shear zones; the northern shear zone separates it from a low pressure/high temperature metamorphic belt consisting of cordierite-bearing garnet sillimanite gneiss and two-pyroxene granulite (Li and Zhang, 2004), and the southern from a unit of interlayered marble and chlorite–white mica schist (Zhang et al., 2008a). The blueschist– eclogite belt consists of eclogite, blueschist, phengite schist and greenschist associated with serpentinized ultramafic rocks (Gao et al., 1999; Klemd et al., 2002; Zhang et al., 2007). Eclogite and blueschist mainly occur as lenses and blocks in prevalent garnet–mica schists, Veins form networks in eclogites and bluschists of centimeter to meter scale. They are composed of omphacite, quartz, epidote, amphibole,carbonate, garnet and rutile in variable modal proportions, P–T estimates vary strongly from 400–600 °C at 1.7–3.2 GPa.

The samples of Meyer et al. (2011) represent ultra-high temperature (UHT) metamorphic rocks from the Epembe Unit of the Epupa Complex in NW-Namibia. The Epupa Complex is exposed in NW Namibia and is situated at the southwestern margin of the Archean to Palaeoproterozoic Congo Craton of central Africa. The rocks of the Epupa Complex were primarily formed during the Eburnian Orogeny which corresponds to a major crust-forming event defined by the formation of Palaeoproterozoic supracrustal rocks and associated synvolcanic and syn- to late kinematic intrusive rocks (e.g. Cahen et al., 1984), The Epupa Complex rocks were

intruded by the Kunene Intrusive Complex (KIC), which is one of the largest massif-type anorthosite bodies in the world, The Epupa Complex is subdivided into the upper amphibolite-facies rocks of the Orue Unit and the UHT granulite-facies rocks of the Epembe Unit, Both units comprise volcano-sedimentary rocks , The E–W-trending Epembe Unit is a granulite-facies fault bounded terrane of 50 km length and up to 10 km width, exposed to the south of the anorthositic KIC. It consists of a metamorphosed volcano-sedimentary sequence, comprising orthogneisses, such as metavolcanic mafic and felsic granulites, and paragneisses, including metagreywackes, metapelites and quartz rich garnet-orthopyroxene rocks. Sapphirine-bearing orthopyroxene sillimanite gneisses and orthopyroxene-garnet rocks occur as rare restitic domains. This volcano-sedimentary sequence is transected by rare granulite-facies garnet-orthopyroxene granitoids and intermediate mafic dikes, which are metamorphosed to mafic granulites (Brandt et al., 2003). The granulite-facies metamorphism is interpreted to result from the accretion of anorthositic melt onto the lower crust. Peak-metamorphic P–T conditions of 9.5±2 kbar and 970 ± 40 °C were estimated by garnet-orthopyroxene Fe-Mg-Al thermometry (Brandt et al., 2003), Subsequent decompression started under UHT granulite-facies conditions and was followed by cooling to amphibolite-facies conditions.

The samples of Şengün et al. (2016) belong to meta-ophiolitic rocks from the Kazdağ Massif, NW Turkey. The Kazdağ Massif lies in the Sakarya Zone and is located in the south of the Biga Peninsula of northwest Turkey. The Kazdağ Massif structurally forms a NE-SW plunging anticlinorium of medium to high-grade metamorphic rocks. The Kazdağ Massif is generally regarded as a Late Oligocene metamorphic core complex (Okay et al. 1991; Okay and Satır 2000). The medium-grade metamorphic basement rocks of the Kazdağ Massif are mainly composed of felsic gneisses, amphibolite, marble and metaophiolitic rocks at the basal – middle part of the

massif, and metagranite associated migmatite, amphibolite, and marble intercalations at the top. The meta-ophiolitic rocks of the Kazdağ Massif occur in the core of the anticlinorium, The meta ophiolitic rocks, a typical oceanic assemblage, consist of meta-ultramafic rocks and dark-green coloured, banded meta-gabbro .The metamorphic rocks of the Kazdağ Massif underwent amphibolite to granulite-facies metamorphism under progressive compression during the Alpine orogeny. The P-T conditions of metagabbros were estimated to be 639 to 662 °C and 9 kbar.

Results

Ti in zircon thermometer

Temperatures were calculated using Ti in Zircon thermometer by Waston et al. (2006) based on the Ti concentration of the samples. Samples of Mitchell (2018) (EGB-09-45), Korhonen (2014) (EGB-09-38,EGB-09-39) and Ewing (2013) (IVT 20) were used to calculate the temperatures. ., Samples of Mitchell (EGB-09-45) and Korhonen (EGB-09-38, EGB-09-39) represented UHT metamorphic rocks with temperature calculated from conventional geothermometers exceeding 950°C whereas sample from Ewing (2013) ranges between 950-900°C from conventional thermometer. (Fig 1.a,b,c)and table shows that EGB-09-45 yield maximum ranging from ~790-950°C whereas EGB-09-38 and EGB-09-39 show slightly lower temperatures (750-915°C). All these samples reach or exceed the initial boundary of the UHT realm. The results of the IVT 20 (Fig 1.d) show much lower temperature, mostly clustered between 700-810°C with few data reaching up to 900°C.

Zr in rutile thermometer

Then we calculated the temperature using the Zr in Rutile thermometer both by Watson et al. (2006) and the one calibrated by Tomkins et al. (2007) for Beta Quartz field at 8 kbar pressure. (Fig 2.a) Samples of Ewing et al. (2013) were used (IVT 01, 20, 31, 32, 33, 34, 36, 37, 38, 39, 40, 42, 43) were used. Both the thermometers shows rise in temperature with rise in Zr concentration and gives temperatures up to >1200°C. At lower concentration of Zr (<5000ppm) both of the

thermometers shows nearly similar temperatures but at higher Zr concentration thermometer by Watson et al. (2006) shows slightly higher temperature. To observe the pressure effect on the Zr in Rutile thermometers samples of Ewing et al. 2013 were used (IVT 01,20,31,32,33,34,36,37,38,39,40,42,43) and the calculations were done in the beta quartz field according to Tomkins (2007) using different pressure of 6,8,10,12 kbar(Fig 2.c) The results show that temperature increase with increasing pressure and the variation of temperature for individual points varies within 50°C between 6-12 kbar. The results are compared with the results yielded by the calibration of Watson (2006) for the same set of samples and it shows that at low pressure (6 kbar) Watson (2006) yields slightly higher temperature than that of Tomkins (2007). At higher pressure (12 kbar) the calibration of Tomkins (2007) yields higher temperature than that of Watson (2006). At 8-10 kbar pressures the results of both the calibrations become very much similar.

We then calculated the temperatures using Zr in rutile thermometer calibrated by Tomkins et al. (2007) for alpha, beta, coesite field by increasing the pressure from 0-30 kbar and by keeping the Zr concentration fixed at 200,500,1000,1500,2000,5000 ppm,(Fig 3.a-f). Temperature by Zr in Rutile thermometer of Watson et al. (2006) was also plotted along with these results. The figure shows that the thermometer calibrated within the alpha and beta quartz field showing similar temperatures for all the Zr contents. These thermometers are also is more pressure sensitive than the coesite field thermometer.The coesite field thermometer is showing higher temperature in all the cases to a certain pressure after which the temperatures of alpha, beta thermometers coincide or in some cases exceeds that of the and coesite field. This inflection depends on the Zr concentration. At low Zr content (200-500 ppm) the inflection occur at 25kbar and above that beta quartz thermometer yields highest temperature compared to other thermometers. At higher concentration of zircon (1000-5000 ppm) the inflection occur at 30 kbar. Comparing with the

results of Wastson et al. (2006) thermometer for Zr in Rutile we see that at 10-12 kbar the alpha, beta thermometers and Watson (2006) show similar temperatures. Below that pressure results of Watson (2006) shows higher temperature and above that pressure thermometer of Watson (2006) shows lower temperatures. The coesite field thermometer always shows higher temperature than that of the Watson (2006).

Comparison of the thermometer

Using the available data of samples (IVT 01, IVT 20) from Ewing et al. (2013) and from Liu et al. (2015) (03LT1-1,03LT3-2,07LT6-1) results from both the thermometers were compared(Fig 4.a). We used the calibration by Watson et al. (2006) for Ti in Zircon thermometer and for Zr in Rutile thermometer calibration by Tomkins (2007) for beta quartz field at 8 kbar pressure were used .The results show that some of the temperatures plot within ±100°C and some within and outside ±200°C. For IVT20 all the temperatures are plotted within the ±100°C and therefore, they provide most consistent results. However, results of samples from Liu et al. (2015) show that Ti in Zircon thermometer yield very low temperature compared to the Zr in Rutile thermometry. For most of the samples, Zr in rutile temperatures is 150-200°C higher than Ti-in-zircon temperatures. Some of the samples are showing opposite results.

Zr in rutile Thermometry for different metamorphic grade rocks

To understand the limitation and application of the accessory phase thermometers we calculated the temperatures from rocks of different metamorphic grades.

Samples from Spear et al. (2006) represents blueschist grade of rocks. Conventional geothermobarometry suggest that the peak metamorphic conditions attained at 475°C with a

variable pressure range from 12-18 kbar (Spear et al. 2006). Zr in Rutile temperatures are calculated using the calibration of Watson et al. (2006),calibration of Tomkins et al. (2007) for alpha, and beta quartz field at 8, 12, 18 kbar (Fig 5.a) . We see that at lower pressure, temperature from Tomkins (2007) at 8 kbar shows the lowest temperatures (450-510°C) which matches well with the previously documented temperatures from geothermometer(Fig 5.b). At higher pressure i.e. 12-18 kbar the temperatures range between 470-525°C and 495-550°C which is slightly higher than that found in conventional approach. Temperature from Watson (2006) range between 450-505°C which is more or less similar to that of the previously recorded temperatures.

For amphibolite facies rocks, temperatures were calculated using Wastson et al. (.2006) thermometer and Tomkins (2007) Zr in rutile thermometer calibrated for beta quartz field at 9 kbar pressure. Data from Şengün et al. (2016) were used to constrain these temperatures(Fig 6.a). ,Conventional geothermobarometry yielded a P-T of 640-660°C at 9 kbar pressure. Zr-in-rutile thermometer of Watson (2006) show temperature range in 600-700°C which is similar to the temperatures calculated from that of Tomikns (2007). Although these temperatures overlap with the temperature range of independent thermometers, accessory phase thermometer shows a much wider range.(Fig 6.b)

Samples of Meyer et al.2011 represent ultra high temperature granulite grade metamorphism as independent geothermobarometers yield P-T range of 970°C and 9.5 kbar and Zr-in-rutile temperatures were calculated using Watson et al . (2006) thermometer and Zr in rutile thermometer of Tomkins (2007) calibrated for beta quartz field at 9.5 kbar pressure. Both the thermometers shows nearly identical temperatures ranging from 350-990°C(Fig 6.c).Pressure Temperature plot was also made to see the zircon spread and comparing with the independent geothermobarometry

both the thermometers shows wide range of temperature with dome data showing very low temperatures(Fig 6.d).

For eclogite facies samples from Chen et al. (2013) were used. ,Temperatures were calculated using Wastson et al .(2006) thermometer and Zr in rutile thermometer of Tomkins (2007) calibrated for beta quartz field (at 10,15,20 kbar) and coesite field (at 27kbar)(Fig 5.c). P–T estimates independent geothermobarometry vary from 400–600 ^{o}C at 17–32 kbar. (Fig 5.c) also shows that the results from the Watson (2006) and that of the Tomkins (2007) at 10 kbar show more or less similar temperature with the previously documented results. However at higher pressure thermometer of Tomkins (2007) yield higher temperature ranging from (530-780°C). In the pressure temperature plot comparing the spread with independent thermometer all the thermometers i.e. of Watson(2006) and Tomkins (2007) (at pressure 10,15,20 kbar) shows higher temperatures.(Fig 5.d)

Ti in zircon Thermometry for different metamorphic grade rocks

The temperatures from Ti in Zircon thermometer using the calibration of Watson et al. (2006) have been compared for different metamorphic facies rocks like granulite, low temperature eclogite and eclogite facies. For granulite facies samples of Qiao et al. (2016) were used (HLO1-1, HL36-6,QL68-2) to calculate temperatures using Ti in Zircon thermometer. Independent geothermobarometers show that the assemblage that the rocks were subjected to 9.3–9.7 kbar/656–674◦C metamorphism followed by an increase in P-T conditions reaching up to 850–870◦C and 14–15 kbar. Results ,show that we see some of the data points yield temperature >900^{o}C reaching upto UHT conditions. However, most of the data show very low temperatures reaching up to 650°C.(Fig 7.c)

For low temperature eclogites samples were taken from Lin et al. (2018) to calculate temperature by Ti in Zircon thermometer by Watson et al. (2006)., Figure 7.a show wide range of temperature from >600 ^{o}C to near about 900^{o}C. In plotting the pressure-temperature plot and comparing with independent geothermobarometry we see that the Ti in Zircon thermometer shows significantly high temperatures.

For samples that were taken from Liu et al. (2015) for eclogites to calculate temperature by Ti in Zircon thermometer by Watson et al. (2006). The metamorphic PT conditions for the samples were found to be 22–26 kbar and 460–510°C. ,Figure 7.b show a wide temperature range from 600 to about 1200^{o}C (reaching up to UHT condition) On comparing with independent geothermobarometry in pressure temperature plot in which temperature spread was plotted at 33kbar. We observe that the Ti in Zircon thermometer shows a wide range and generally shows higher temperatrures compared to independent thermometry with some data showing similar and some showing lower temperatures.

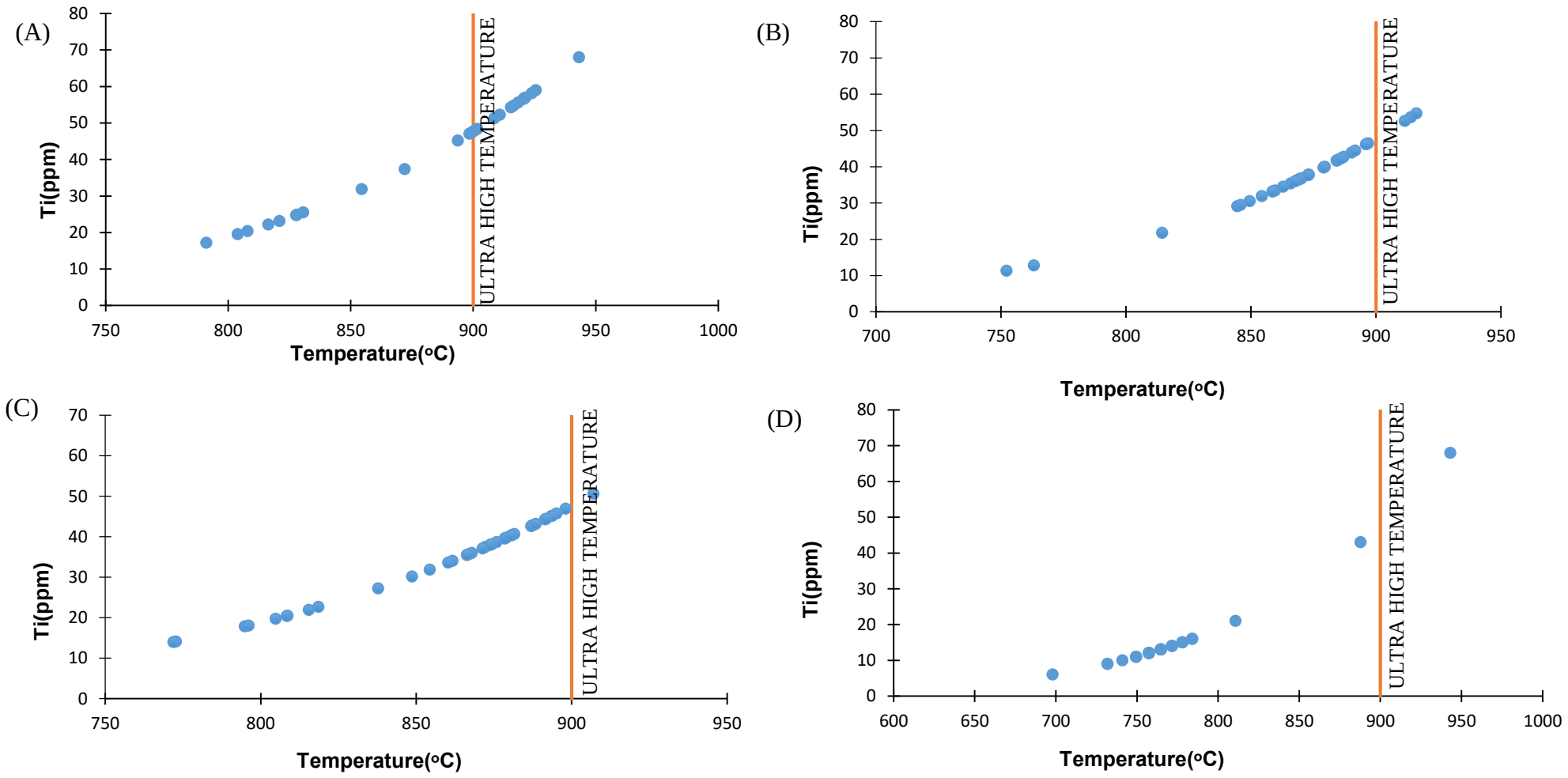

Fig 1 Ti in Zircon temperature calculated using calibration of Watson 2006 A)Temperatures calculated using sample of Mitchell 2018 (EGB-09-45),B,C)Samples of Korhonen 2014 were used(EGB-09-38,EGB-09-39) to find the temperatures,D)Samples of Ewing 2013 was used for estimating temperatures(IVT-20)

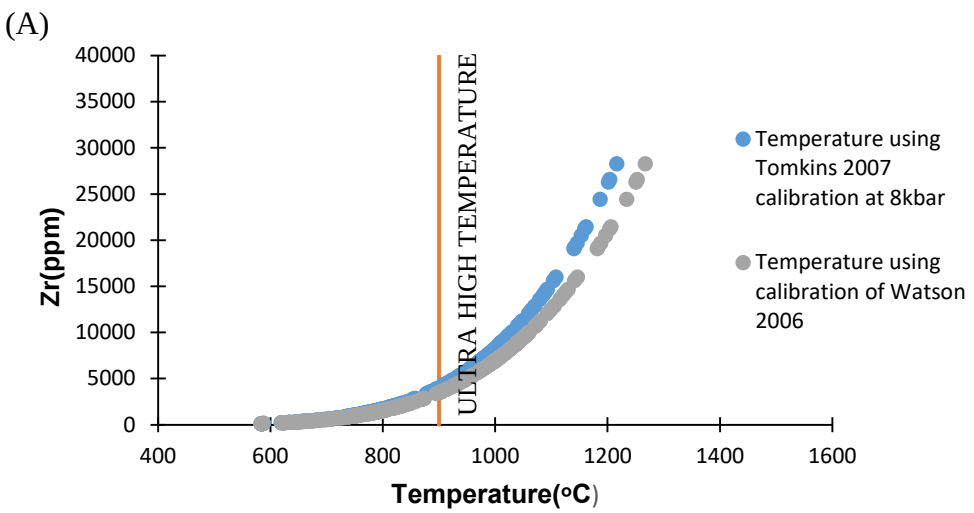

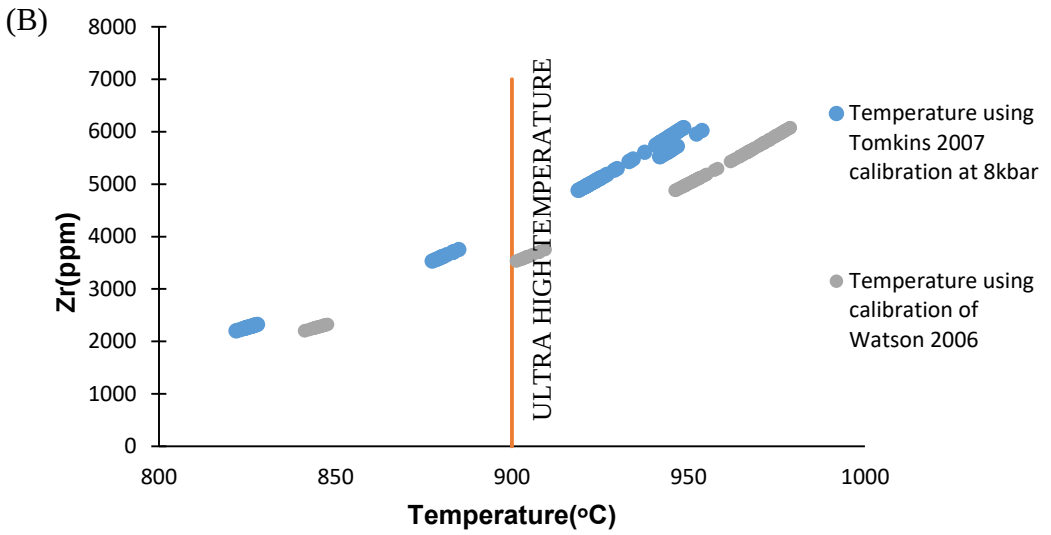

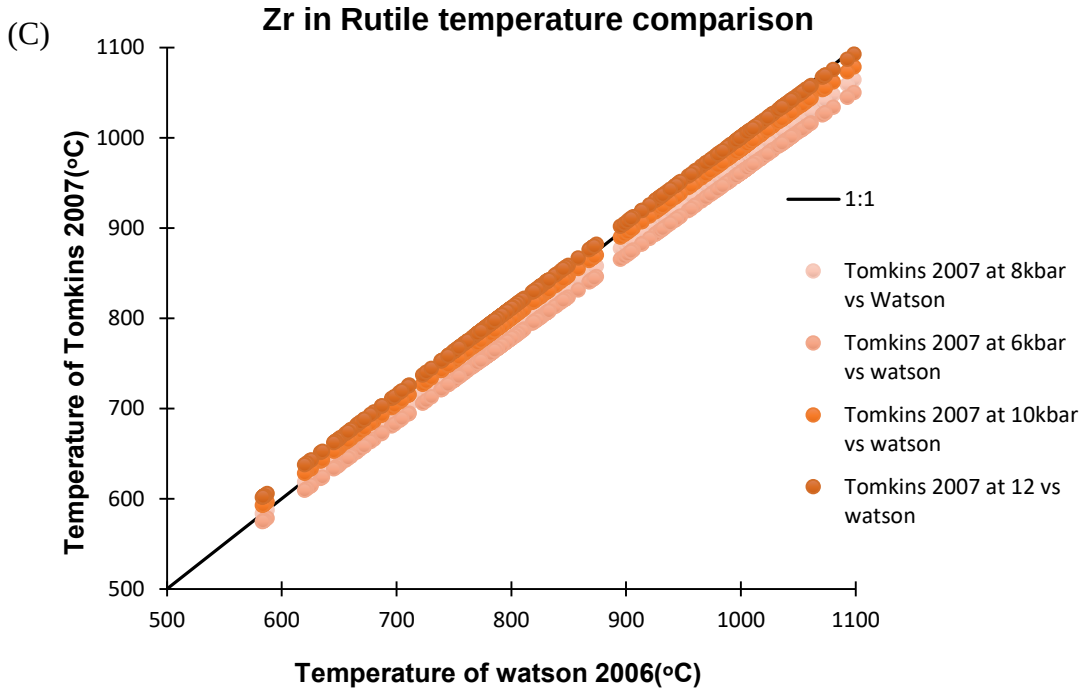

Fig 2 A)Zr in Rutile temperature estimated using calibration of Tomkins 2007 for beta quartz field at 8kbar and calibration of Watson 2006,samples of Ewing 2013 were used to find the temperatures B)Samples of Korhonen 2014(EGB-09-38,EGB-09-39) were used to find the temperatures using the above said calibrated thermometers C)Comparison of temperatures between calibration of Watson 2006 and calibration of Tomkins 2007 for beta quartz field at 6,8,10,12kbar using samples of Ewing 2013

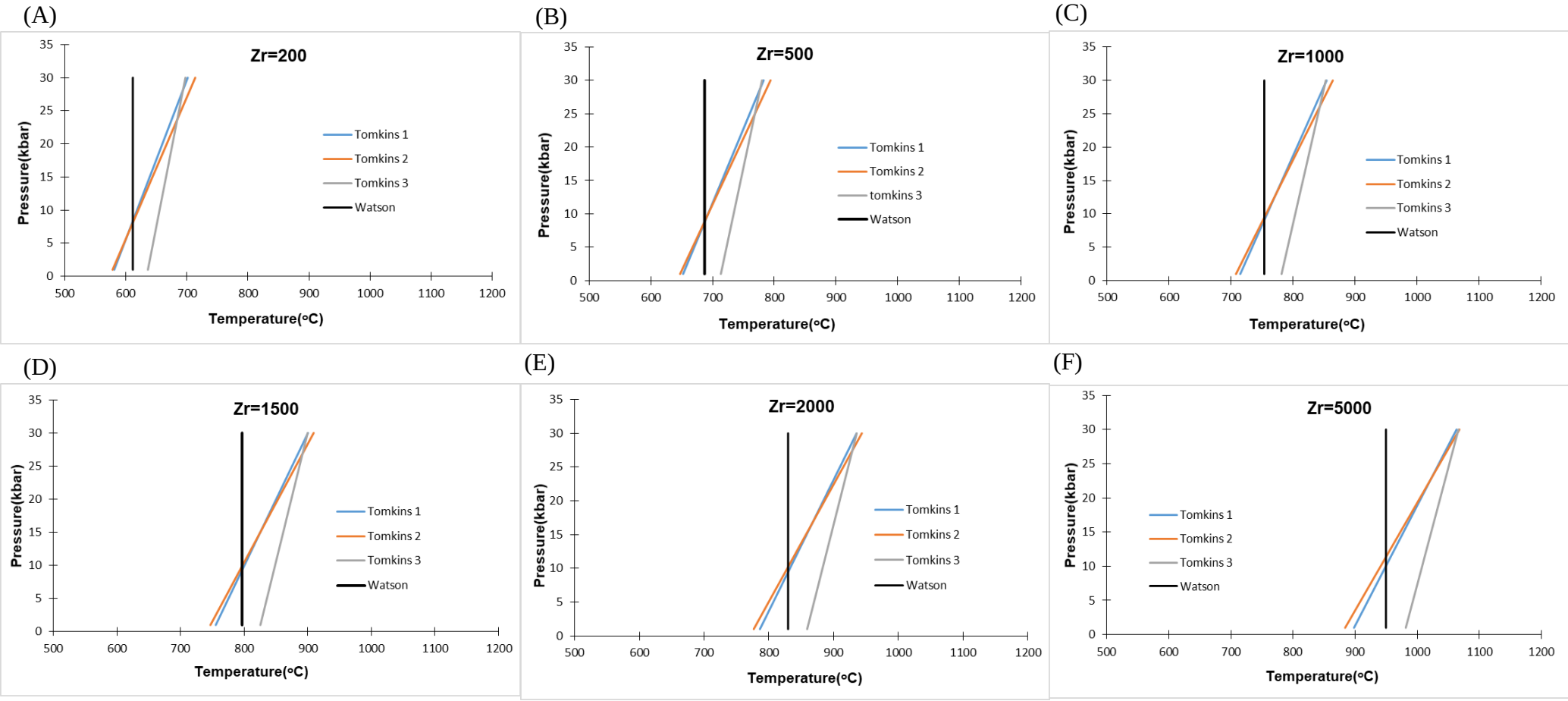

Fig 3 Tomkins 1,2,3 refers the three calibration of Tomkins 2007 for alpha,beta quartz and coesite field respectively A,B,C,D,E,F)Zr in Rutile temperatures calculated using calibration of Tomkins 2007 for alpha ,beta quartz and coestite field and calibration of Watson 2006 for different Zircon concentrations namely 200,500,1000,1500,2000,5000ppm along with rising pressures

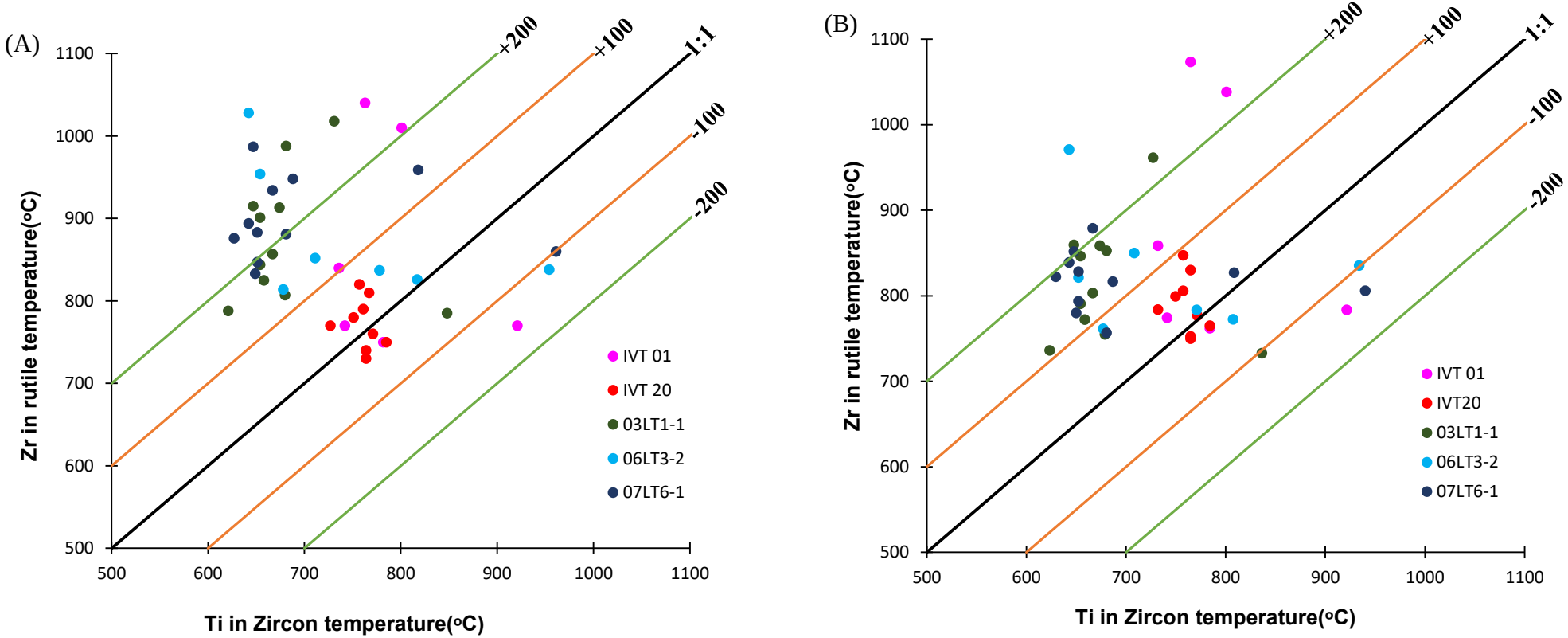

Fig 4 A)Comparison of Ti in Zircon temperature estimated using calibration of Watson 2006 and Zr in Rutile temperatures estimated by calibration of Tomkins 2007 using samples of Ewing 2013(IVT-01,IVT-20) and Liu 2015(03LT1-1,06LT3-2,07LT6-1). B)Comparison of Ti in Zircon temperatures and Zr in rutile temperatures using calibration of Watson 2006 for the above mentioned sampkes.

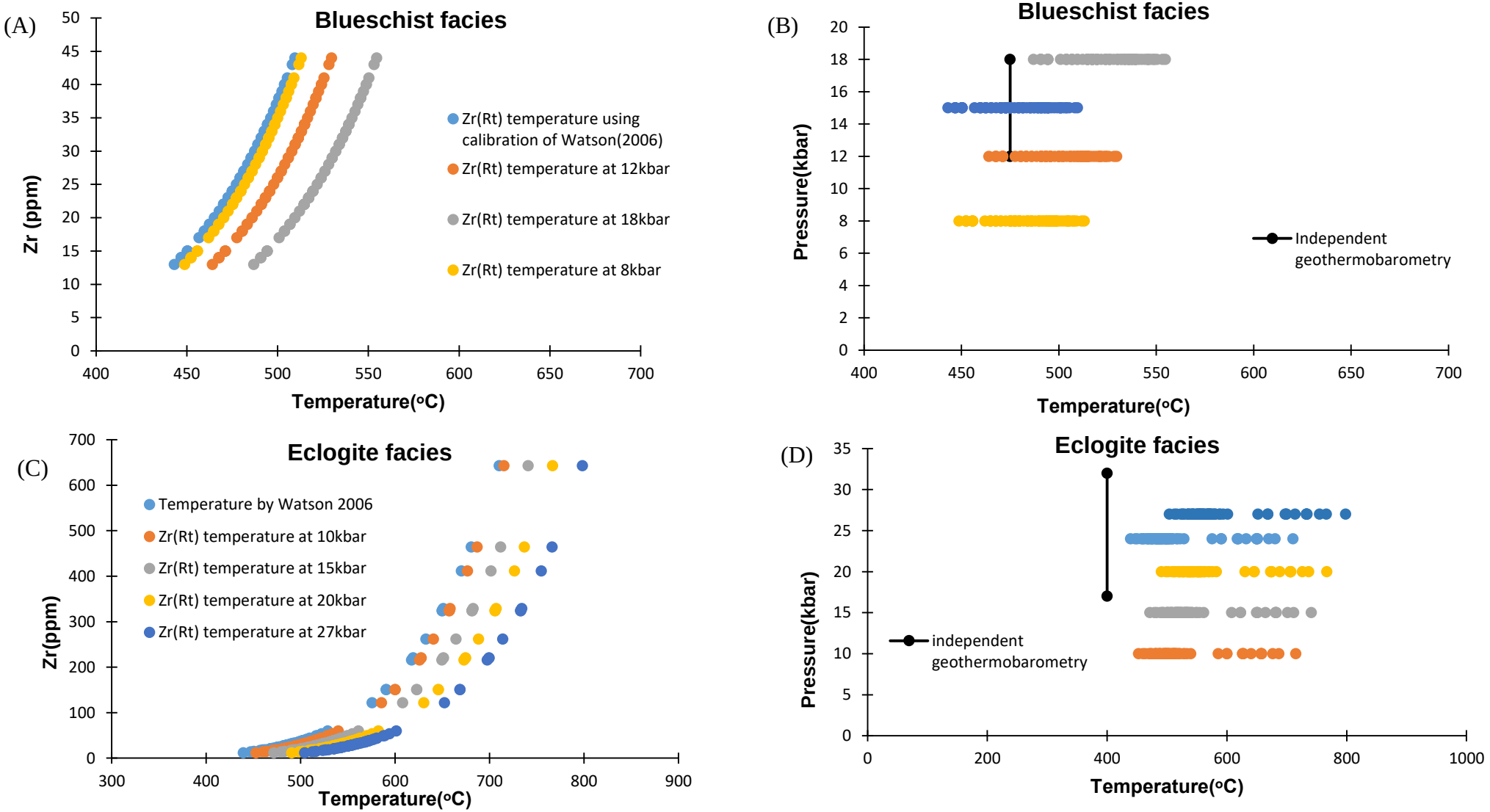

Fig 5 A) Zr in Rutile temperature calculated using calibration Watson 2006 and calibration of Tomkins 2007 for beta quartz field at 8,12,18kbar for blueschist facies rocks using samples of Spear 2006 B)Comparison of temperatures with that of independent geothermobarometry for blueschist facies C) Zr in Rutile temperature calculated using calibration Watson 2006 and calibration of Tomkins 2007 for beta quartz field(10,15,20kbar) and coesite field(27 kbar for eclogite facies rocks using samples of Chen 2013 D) B)Comparison of temperatures with that of independent geothermobarometry for Eclogite facies

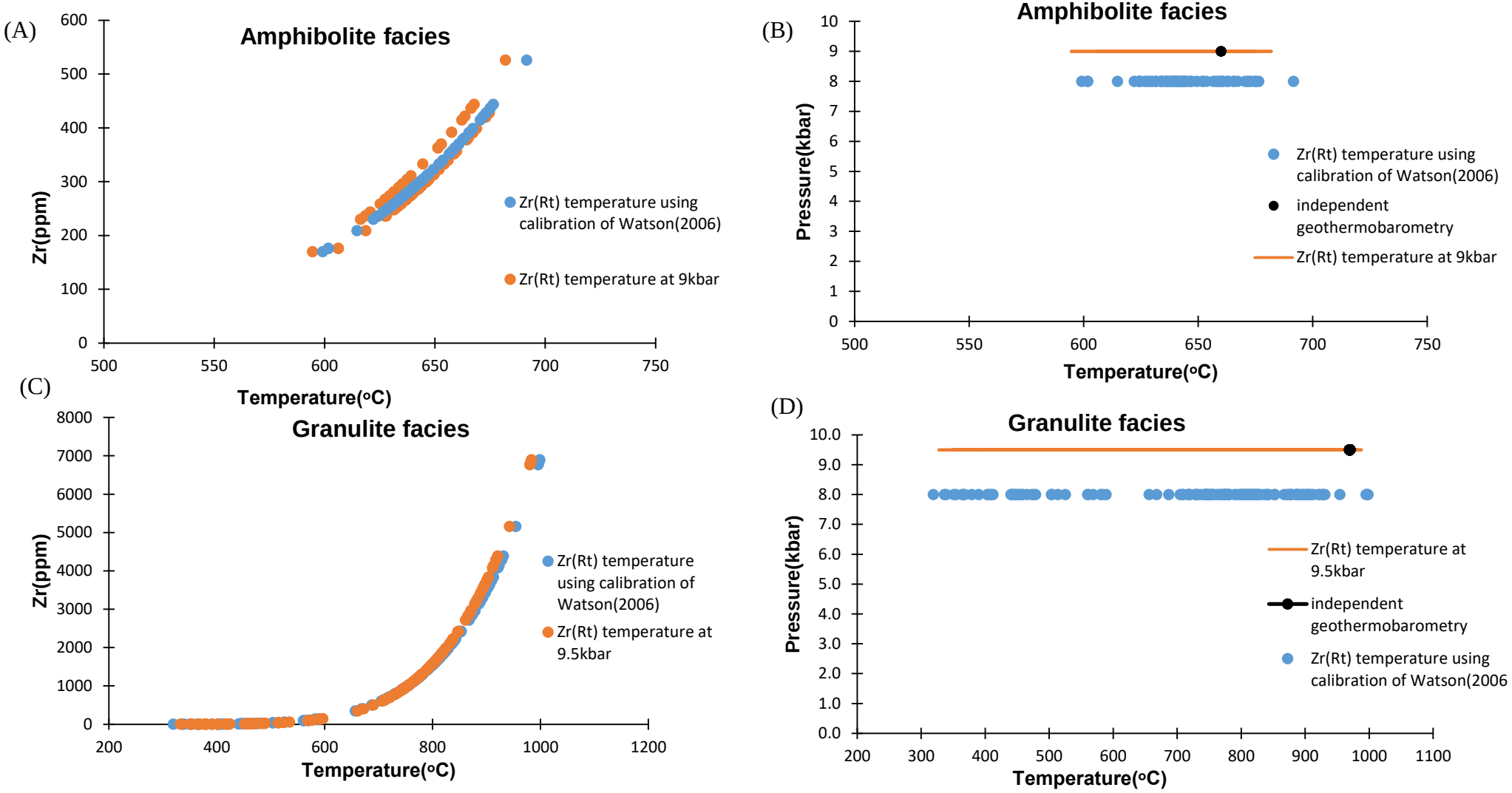

Fig 6 A)Zr in Rutile temperature calculated using calibration Watson 2006 and calibration of Tomkins 2007 for beta quartz field at 9kbar for amphibolite facies rocks using samples of Şengün 2016 B)Comparison of temperatures with that of independent geothermobarometry for amphibolite facies C)Zr in Rutilr temperature calculated using calibration of Watson 2006 and calibration of Tomkins 2007 for beta quartz field at 9.5kbar using samples of Meyer 2011 D) B)Comparison of temperatures with that of independent geothermobarometry for granulite facies

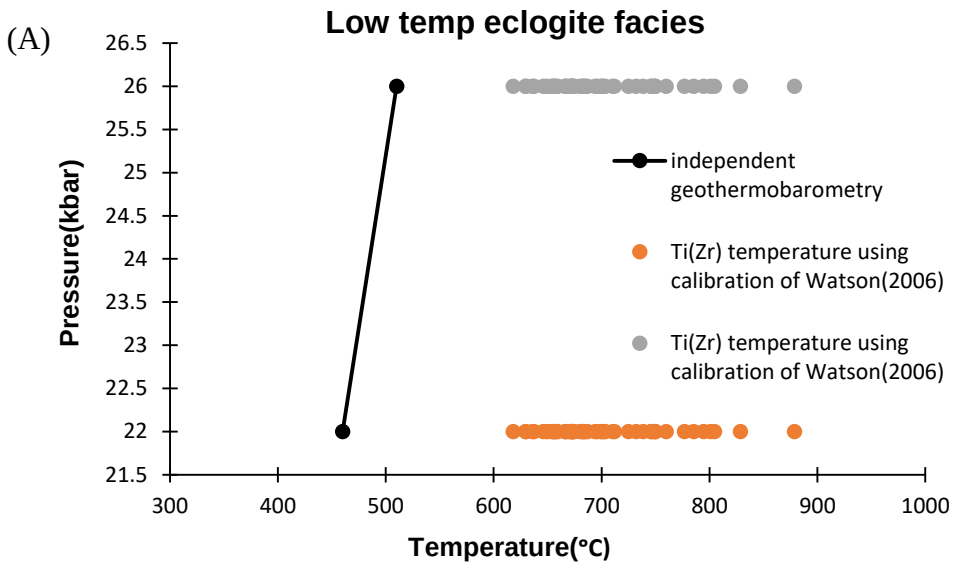

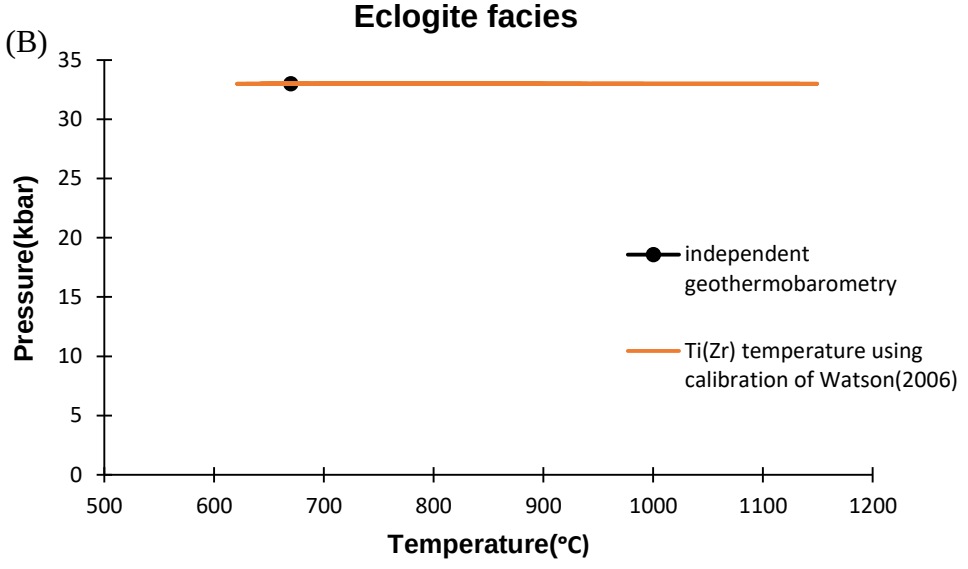

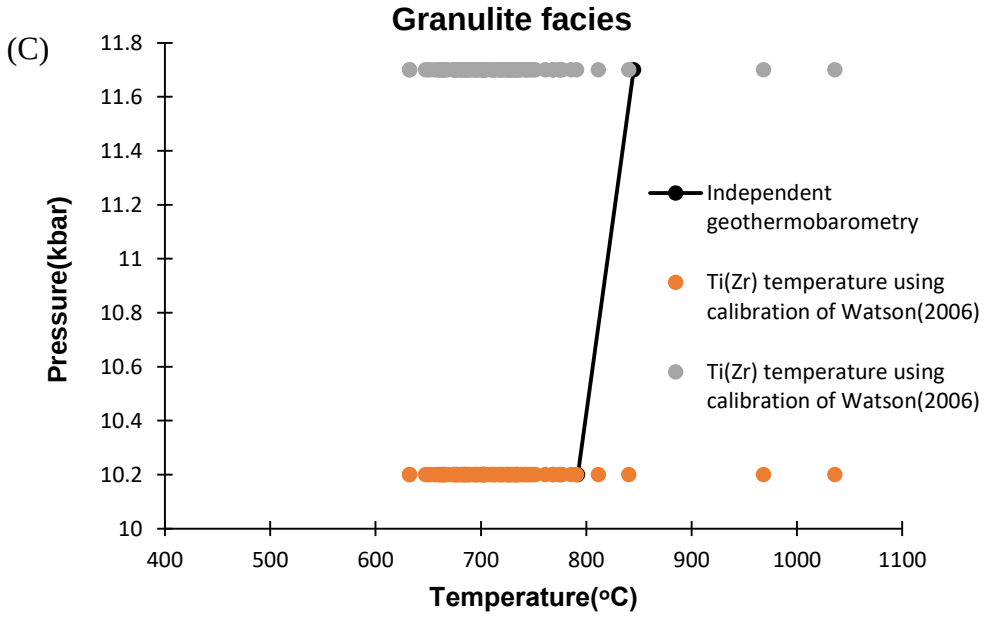

Fig 7 A)Ti in Zircon temperatures were calculated using calibration of Watson 2006 for low twmperature eclogite facies rocks using samples of Lin 2018 and were compared with independent geothermobarometry B)Ti in Zircon temperatures were calculated using calibration of Watson 2006 for eclogite facies rocks using samples of Liu 2015 and were compared with independent geothermobarometry C)Ti in Zircon temperatures were calculated using calibration of Watson 2006 for granulite facies rocks using samples of Qiao 2016 and were compared with independent geothermobarometry

Discussion

In the last decade, trace element accessory phase thermometers have been largely used to constrain the temperatures of different grade of metamorphic rocks of varying lithology and ranging over wide temperatures. Zr-in-rutile thermometry has been considered as one of the robust thermometers especially for granulite grade rocks (Horton et al., 2016; Holder, & Jöns, 2016; Korhonen et al., 2014; Taylor et al., 2016). However, as stated by Watson (2006) and Tomkins (2007) that these thermometers have certain limitations and there exists some situations when the results of the thermometers proved to be ambiguous. This study evaluates the applicability of the thermometers using the natural examples.

The results of this study re-affirms that Ti intake in zircon and Zr intake in rutile strongly depend on the temperature. Watson et al (2006) suggested that Ti in zircon thermometer is insensitive to pressure. The authors did not observe the systematic effect of pressure on Zr-in-rutile. Citing natural examples they have suggested that pressure has minimal effect on the thermometers. Tomkins (2007) opposed the view and modified the calibration using the effect of pressure. Results from this study show that Zr-in-rutile thermometer indeed produces different temperatures at different pressures. However, from 6-18 kbar pressure the results do not show any significant deviation and are similar within ±50°C. In his study, Watson (2006) used experiments and natural examples having a large pressure range varying from 10-20 kbar. Results of the Zr-in-rutile thermometry using the calibration of Watson (2006) matches well with the results of the thermometry of Tomkins (2007) only upto10 kbar pressure.

Effect of pressure

Zr in Rutile thermometer calibrated for alpha and beta quartz field of Tomkins et al. (2007) shows more or less similar temperature and is more pressure sensitive than the thermometer for coesite field (>=27kbar). Zr-in-rutile thermometry in alpha and beta quartz yield low temperatures than coesite field thermometer. So using either alpha or beta quartz thermometers will provide similar results, whereas using the coesite field thermometer below 27 kbar will give unusually high temperatures. It has also been observed that coesite field thermometer is less sensitive to pressure compared to other two thermometers. Exact reason of this phenomenon has not been explained but the fact that compressibility of rutile at high pressure (Tomkins 2007) it is likely that the thermometer will be less sensitive at high pressures. However, it seems likely that for low pressure rocks (<10kbar), Zr-in-rutile thermometer calibrated for both alpha and beta quartz field by Tomkins et al (2007) and by Watson (2006) can be used. For moderate pressure rocks the calibration of Tomkins et al (2007) for both alpha and beta quartz field should be used rather than that of Watson (2006). For high pressure rocks coesite field Zr-in-rutile thermometer can be used to get reliable temperature estimates.

Comparison of the Zr-in-rutile and Ti-in-zircon thermometers

It has also been intriguing that the results of the Ti-in-zircon thermometry and the Zr-in-rutile thermometry yield significant variation in temperature irrespective of rocktype and P-T regime. The calibration of Tomkins (2007) for Zr-in-rutile thermometer always shows 100-200°C higher temperature than the Ti-in-zircon thermometers. Even when two thermometers are calibrated by Watson (2006), Zr-in-rutile show 50-100°C higher temperature values than the Zr-in-rutile. These observations were also corroborated by several authors (viz. Clarke et al., 2019). Fu et al. (2008)

compared the crystallisation temperatures of mafic rocks and Ti-in-zircon thermometers to evaluate its limitation and they also found that this thermometer systematically produces low temperatures. The calculations used in this study also show that Ti-in-zircon thermometry show a large range of temperatures which is often lower than the temperatures determined from independent thermometers and in some cases they are unusually low (~350°C). Fu et al. (2008) suggested that apart from the temperature and TiO2 activity, Ti content of zircon is influenced by the activity of SiO2 and pressure. For the metamorphic rocks it has been suggested that rutile often forms at the peak metamorphic conditions and is included within other metamorphic phases like garnet (Clarke et al. 2019). The process therefore shields the rutile from subsequent equilibration with other phases. Zircon, on the other hand tends to grow during melt crystallization, and therefore is less likely to record extreme temperature (e.g. Clark et al., 2018; Korhonen et al., 2014). It has also been suggested that zircon in metamorphic rocks may also re-equilibrate in response to changing P–T conditions or fluid compositions (Kooijman et al., 2011). Therefore, highest Ti-in-zircon temperatures recorded in zircon might represent the primary zircon crystallization and the lowest Ti concentrations might record re-equilibration (Timms et al. 2011). Besides, for metamorphic rocks the inclusion of rutile into porphyroblastic phases effectively removes the phases from the equilibration and zircon grains that grow in such conditions equilibrates with *a*TiO2 significantly lower than modeled (Clark et al.2019).

Accessory phase thermometers and HT/UHT metamorphism

Trace element thermometry is believed to be of specific importance because

a) The incorporation of the trace elements in the accessory phases is temperature dependent with minimum effect of pressure

b) Ti^{+4} and Zr^{+4} is believed to have sluggish diffusion rates within the zircon and rutile which inhibits the significant post-peak homogenization of the elements in the phases. The peak temperatures (>850°C) for most of the HT/UHT metamorphic rocks exceed the blocking temperature of most of the conventional thermometers involving Fe-Mg exchange. In this backdrop, slow diffusion of trace element proves to be important (Kelsey and Hand, 2015).

c)Accessory phases often form at different textural assemblages which allow the worker to properly constrain the temperature at different part of a P-T path

However, in my study it has been observed that trace element thermometers are frequently showing low temperatures compared to that of the independent thermometers from HT/UHT rocks. Using the natural examples, Kelsey and Hand (2015) evaluated the applicability of the trace element thermometers for constraining the peak temperatures in HT/UHT metamorphic rocks. Their study matches with our observation that in spite of having the advantages discussed above, a significant number of HT/UHT samples show much low temperatures compared to the HT/UHT regime. Like other examples, Zr-in-rutile frequently records hgher temperatures than that of Ti-in-zircon in the granulite grade conditions. Apart from the reasons discussed in above section, there are certain explanations to this fact as argued by Kelsey and Hand (2015)

i) Rutile is often stable before and during the attainment of peak conditions (Kooijman et al., 2012) whereas zircon usually began to form at the peak as a result of which Ti-in-zircon temperatures represent close-to-solidus temperatures along with the retrograde part of the P-T path (Brown and Korhonen, 2009; Korhonen et al., 2013);

ii) Ewing et al., (2013) suggested that unlike zircon, rutile is less susceptible to post peak retrogression and alteration in UHT rocks.

iii)In granulite grade rocks, Zr content in rutile is usually higher than Ti content in zircon which makes the former less susceptible to analytical error.

iv) Rutile grains in granulite are usually larger than that of the zircons which makes the former resistant to complete homogenization during post-peak diffusion.

In this backdrop it seems likely that Zr-in-rutile provide more robust thermometry for HT/UHT rocks than Ti-in-zircon thermometer does. However, my study reveals that Zr-in-rutile thermometer can also produces lower temperatures than of the independent thermometers.

Possible reasons could be the recrystallization of rutile under decompressional granulite-facies conditions and fluid-mediated recrystallization during the subsequent amphibolite facies retrogression.(Meyer et al. 2011) as the apparent closure temperature of rutile for volume diffusion of Zr ranges between 560 and 730 °C for grains with a diameter of 100 μm (Watson et al., 2006).

Conclusions

The study shows that the results of the trace element exchange thermometry involving zircon and rutile, are sensitive to several factors and most importantly should be used only for appropriate assemblages (for Ti-in-zircon in presence of rutile and for Zr-in-rutile, in presence of zircon and quartz). Apart from the temperature and concentration of trace elements in in the rock, the intake of trace element in the accessory depends on pressure and SiO2 activity. Besides post-peak retrogression and alteration have significant influences on the results of the thermometers. Although the effect of pressure is not well documented for the Ti-in-zircon thermometers, Zr-in-rutile thermometer is sensitive to pressures. The results at low pressures calibrated by Tomkins (2007) commonly overlaps with that of the Watson (2006). However, the effect of pressure on the

thermometer is more dramatic above the pressure 25 kbar, in the coesite field. Concentration of Zr does not significantly affect the results of the thermometry provided by different calibrations.

The results show that for same samples, Zr-in-rutile thermometer commonly provides higher temperatures than that of the Ti-in-zircon. The variation is more pronounced in case of HT/UHT metamorphic rocks. The major reasons incudes lowering of aTiO2 when rutile gets shielded by porphyroblastic phases, formation of rutile in pre to syn-peak conditions, low probability of rutile being altered to post-peak retrogression. In this backdrop, Zr-in-rutile appears to be more robust thermometer than Ti-in-zircon. This study also reveals that Zr-in-rutile thermometry often shows wide temperature ranges that are different than the other temperature estimates which is also consistent with the results from other studies (Usuki et al., 2017. JP; Harley,2016). Therefore, it seems likely that trace element accessory thermometers have certain limitations than previously thought and can only be used with the support of other independent thermometers.

Acknowledgement

It is a matter of great pleasure for me to offer my sincere gratitude and cordial thanks to all the persons whose immense help has made this learning experience truly impounding. I am thankful to Department of Geological Sciences, Jadavpur University for providing all possible cooperation and necessary infrastructural facilities.

First of all I want to express my heartfelt thanks and deepest regards to Prof. Pulak Sengupta ,Department of Geological Sciences,Jadavpur University,under whose guidance this thesis work has been carried out. His kind supervision, valueable guidance, cooperation, suggestion and discussion at every stage have made this thesis work possible.

I would like to extend my thanks to Dr. Subham Mukherjee for his kind help and cooperation ,without him the dissertation would have been incomplete.

References

1. Watson, E. B., Wark, D. A. & Thomas, J. B., 2006. Crystallization thermometers for zircon and rutile. Contributions to Mineralogy and Petrology, 151, 413–433.
2. Zack T, Moraes R, Kronz A (2004) Temperature dependence of Zr in rutile: empirical calibration of a rutile thermometer. Contrib Mineral Petrol 148:471–488.
3. Tomkins, H. S., Powell, R. & Ellis, D. J., 2007. The pressure dependence of the zirconium-in-rutile thermometer. Journal of Metamorphic Geology 25, 703–713.
4. Liu, Y.-C., Deng, L.-P., Gu, X.-F., Groppo, C., Rolfo, F., 2015.Application of Ti-in-zircon andZr-in-rutile thermometers to constrain high-temperature metamorphism in eclogites from the Dabie orogen, central China. Gondwana Research 27, 410–423.
5. Mitchell, R.J., Johnson, T.E., Clark, C., Gupta, S., Brown, M., Harley, S.L. and Taylor, R. (2018) Neoproterozoic evolution and Cambrian reworking of ultrahigh temperature granulites in the Eastern Ghats Province, India. Journal of Metamorphic Geology, 37, 000–000.
6. Korhonen, F.J., Clark, C., Brown, M. and Taylor, R. (2014) Taking the temperature of Earth's hottest crust. Earth and Planetary Science Letters, 408, 341–354.
7. B. Fu, F.Z. Page, A.J. Cavosie, J. Fournelle, N.T. Kita, J.S. Lackey, S.A. Wilde, J.W. Valley Ti-in-zircon thermometry: applications and limitations Contributions to Mineralogy and Petrology, 156 (2008), pp. 197-215
8. T.A. Ewing, J. Hermann, D. RubattoThe robustness of the Zr-in-rutile and Ti-in-zircon thermometers during high-temperature metamorphism (Ivrea–Verbano Zone, northern Italy) Contributions to Mineralogy and Petrology, 165 (2013), pp. 757-779

9. Chris Clark,| Richard J. M. Taylor, Tim E. Johnson, Simon L. Harley,Ian C. W. Fitzsimons, Liam Oliver(2019) Testing the fidelity of thermometers at ultrahigh temperatures, Journal of Metamorphic Geology, DOI: 10.1111/jmg.12486
10. H.Z. Qiao, C.Q. Yin, Q.L. Li, X.L. He, J.H. Qian, W.J. LiApplication of the revised Ti-in-zircon thermometer and SIMS zircon U-Pb dating of high-pressure pelitic granulites from the Qianlishan-Helanshan Complex of the Khondalite Belt, North China Craton Precambr. Res., 276 (2016), pp.1-13
11. LIN, M., ZHANG, G., SONG, S., LI, H. & ZHANG, L. 2018. The validity of Ti-in-zircon thermometry in low temperature eclogites. In: ZHANG, L.F., ZHANG, Z., SCHERTL, H.-P. & WEI, C. (eds) HP–UHP Metamorphism and Tectonic Evolution of Orogenic Belts. Geological Society, London, Special Publications, 474. First published online September 14, 2018, https://doi.org/10.1144/ SP474.13
12. Meyer,M.,John,T.,Brandt,S.,Klemd,R.,2011.Trace element composition of rutile and the application of Zr-in-rutile thermometry to UHT metamorphism(Epupa Complex,NW Namibia).Lithos 126,388-401
13. Chen, Z.Y., Zhang, L.F., Du, J.X. & Lü, Z., 2013. Zr-in-rutile thermometry in eclogite and vein from southwestern Tianshan, China. Journal of Asian Earth Sciences, 63, 70–80
14. Spear FS, Wark DA, Cheney JT, Schumaker JC, Watson EB (2006) Zr-in-rutile thermometry in blueschists from Sifnos, Greece. Contrib Mineral Petrol 152:375–385
15. F. Sengun, T. Zack Trace element composition of rutile and Zr-in-rutile thermometry in meta-ophiolitic rocks from the Kazdag Massif, NW Turkey Mineral. Petrol., 110 (2016), pp. 547-560

16. Kelsey DE, Hand M. On ultrahigh temperature crustal metamorphism: phase equilibria, trace element thermometry, bulk composition, heat sources, timescales and tectonic settings. Geoscience Frontiers 2015; 6: 311–56.
17. T. Usuki, Y. Iizuka, T. Hirajima, M. Svojtka, H.-Y. Lee, B.-M. Jahn Significance of Zr-in-rutile thermometry for deducing the decompression P–T path of a garnet–clinopyroxene granulite in the Moldanubian Zone of the Bohemian Massif Journal of Petrology, 58 (2017), pp. 1173-1198
18. Harley SL. A matter of time: the importance of the duration of UHT metamorphism. J Mineral Petrol Sci 2016; 111: 50–72.
19. F.J. Korhonen, C. Clark, M. Brown, S. Bhattacharya, R. Taylor How long-lived is ultrahigh temperature (UHT) metamorphism? Constraints from zircon and monazite geochronology in the Eastern Ghats orogenic belt, India Precambrian Research, 234 (2013), pp. 322-350
20. N.E. Timms, et al.Relationship among titanium, rare earth elements, U/Pb ages and deformation microstructures in zircon; implications for Ti-in-zircon thermometry Chemical Geology, 280 (1–2) (2010), pp. 33-46
21. E. Kooijman, D. Upadhyay, K. Mezger, M.M. Raith, J. Berndt, C. Srikantappa Response of the U–Pb chronometer and trace elements in zircon to ultrahigh-temperature metamorphism: the Kadavur anorthosite complex, southern India Chemical Geology, 290 (2011), pp. 177-188
22. Harley, S., and N. Kelly (2007), Zircon: Tiny but timely, Elements, 3, 13–18.
23. Cherniak, D.J., Watson, E.B., 2007. Ti diffusion in zircon. Chemical Geology, 242(3-4): 473-486.

24. Watson EB, Harrison TM (2005) Zircon thermometer reveals minimum melting conditions on earliest Earth. Science 308:841–844

25. Rubatto D, Hermann J. Experimental zircon/melt and zircon/garnet trace element partitioning and implications for the geochronology of crustal rocks, Chemical Geology , 2007, vol. 241 (pg. 38-61).

26. Ferry, J. & Watson, E. B. (2007) New thermodynamic models and revised calibrations for the Ti-in-zircon and Zr-in-rutile thermometers. Contributions to Mineralogy and Petrology, doi.10.1007/s00410-007-0201-0, in press.

27. Ferry, J. M. & Spear, F. S., 1978. Experimental calibration of study of low and high plagioclase feldspars. In: T he Feldspars the partitioning of Fe and Mg between biotite and garnet. (eds MacKenzie, W. S. & Zussman, J.), pp. 162–173. Contributions to Mineralogy and Petrology, 66, 113–117.

Appendix

Table 1: Ti in Zr temperature

Mitchell data		
Sample	Ti(ppm)	T(◦C)
EGB-09-45		
45Z - 2.d	17.2	791
45Z - 3.d	19.6	804
45Z - 4.d	24.8	828
45Z - 5.d	20.4	808
45Z - 6.d	22.2	816
45Z - 7.d	25.5	831
45Z - 8.d	59	925
47AZ - 1.d	52.3	911
47AZ - 10.d	54.7	916
47AZ - 11.d	56.6	920
47AZ - 12.d	47.1	898
47AZ - 13.d	56.7	921
47AZ - 2.d	58.2	924
47AZ - 3.d	51.3	909
47AZ - 4.d	55.6	918
47AZ - 5.d	54.3	915
47AZ - 6.d	48.1	901
47AZ - 7.d	56.8	921
47AZ - 8.d	45.2	894
47AZ - 9.d	37.4	872
47B Z - 1.d	24.9	828
47B Z - 10.d	23.2	821
47B Z - 11.d	47.6	900
47B Z - 2.d	57	921
47B Z - 3.d	48.4	902
47B Z - 4.d	68	943
47B Z - 5.d	31.9	854
47B Z - 7.d	390	1213

IVT 20		
SAMPLE	Ti(ppm)	T(◦C)
216ivt20	13	765
217ivt20	12	757
218ivt20	16	784
219ivt20	14	772
221ivt20	9	732
222ivt20	11	749
223ivt20	13	765
225ivt20	13	765
228ivt20	12	757
229ivt20	14	772
230ivt20	15	778
231ivt20	6	698
232ivt20	12	757
233ivt20	16	784
234ivt20	68	943
235ivt20	10	741
236ivt20	12	757
237ivt20	13	765
240ivt20	12	757
242ivt20	15	778
243ivt20	11	749
246ivt20	12	757
247ivt20	9	732
252ivt20	43	888
253ivt20	15	778
255ivt20	14	772
257ivt20	11	749
259ivt20	21	811
260ivt20	13	765

Korhonen data		
Sample	Ti(ppm)	T(◦C)
SAMPLE EGB-09-38		
38-1.1	40	880
38-1.2	42.52	887
38-11.1	42.71	887
38-12.1	53.67	914
38-13.1	30.49	850
38-14.1	52.6	912
38-15.1	41.7	884
38-15.c	37.73	873
38-16.1	33.13	859
38-17.1	33.45	860
38-18.1	37.67	873
38-19.1	36.79	870
38-2.1	46.49	897
38-20.1	33.2	859
38-21.1	36.47	869
38-21.c	37.8	873
38-22.1	43.91	890
38-23.1	35.4	866
38-24.1	11.34	752
38-3.1	39.81	879
38-4.1	44.47	892
38-5.1	36.54	869
38-5.C	29.11	845
38-6.1	12.79	763
38-6.2	21.8	815
38-7.1	36.16	868
38-8.1	54.68	916
38-9.1	46.17	896
38-c.1	34.46	863
38-C.10	36.67	870
38-C.11	36.73	870
38-C.13	41.71	884
38-C.14	41.95	885
38-C.15A	37.71	873
38-C.15B	29.46	846
38-C.16	42.24	886
38-c.2	46.17	896
38-C.3	31.89	854
38-C.4	39.86	879
38-C.5	36.01	868

Table 1 continued

SAMPLE EGB 09 39

SAMPLE	Ti(ppm)	T(◦C)
39-1.1	34.08	862
39-10.1	27.28	838
39-11.1	38.17	874
39-12.1	19.78	805
39-13.1	46.93	898
39-14.1	36.03	868
39-15.1	21.99	815
39-16.1	37.49	872
39-17.1	45.15	893
39-18.1	42.67	887
39-19.1	14.18	773
39-2.1	40.44	881
39-20.1	50.63	907
39-21.1	38	874
39-22.1	45.78	895
39-23.1	30.23	849
39-3.1	39.75	879
39-4.1	45.23	894
39-5.1	35.53	866
39-6.1	14.05	772
39-7.1	35.84	867
39-8.1	22.68	819
39-9.1	44.35	891
39-C.1	20.54	809
39-C.10	33.65	860
39-C.11	39.59	878
39-C.12	39.68	879
39-C.13	43.22	888
39-C.14	37.17	871
39-C.15	44.48	892
39-C.16	40.68	881
39-C.1B	17.87	795
39-C.1C	18.1	796
39-C.2	35.55	866
39-C.3	40.32	880
39-C.4	20.49	808
39-C.5	42.75	887
39-C.6	43.15	888
39-C.7	31.87	854
39-C.8	38.69	876
39-C.9	38.05	874

IVJ-11

SAMPLE	Ti(ppm)	T(◦C)
003ivj11	20	806
005ivj11	30	848
006ivj11	27	837
007ivj11	36	868
011ivj11	23	820
012ivj11	27	837
013ivj11	15	778
014ivj11	29	844
015ivj11	13	765
273ivj11	50	905
275ivj11	16	784
278ivj11	50	905
280ivj11	17	790
281ivj11	16	784
282ivj11	26	833
283ivj11	21	811

IVT-01

SAMPLE	Ti(ppm)	T(◦C)
263ivt01	9	732
264ivt01	57	921
265ivt01	16	784
266ivt01	10	741
267ivt01	1605	1539
268ivt01	19	801
269ivt01	13	765

Table 2: Zr in Rutie temperature

sample	Zr(ppm)	T(°C)12	T(°C)8	T(°C)10	T(°C)6	Tw(°C)
IVT 01						
025-IVT01	2359	859	835	847	824	850
026-IVT01	1330	796	774	785	763	783
027-IVT01	1087	775	754	764	743	762
028-IVT01	1221	787	765	776	754	774
029-IVT01	8737	1035	1008	1022	995	1037
031-IVT01	8828	1037	1010	1023	996	1038
033-IVT01	10827	1070	1042	1056	1028	1073
035-IVT01	919	759	737	748	727	745
036-IVT01	1232	788	766	777	755	775
IVT 31						
118-IVT31	8617	1033	1006	1020	993	1034
119-IVT31	1397	801	779	790	768	789
121-IVT31	7272	1007	981	994	968	1007
123-IVT31	7215	1006	980	993	966	1006
124-IVT31	9406	1047	1020	1033	1006	1049
125-IVT31	9811	1054	1026	1040	1012	1056
126-IVT31	1424	803	781	792	770	791
127-IVT31	7482	1012	985	998	972	1011
130-IVT31	7311	1008	982	995	968	1008
131-IVT31	7574	1013	987	1000	973	1013
132-IVT31	8090	1023	997	1010	983	1024
133-IVT31	9088	1041	1014	1028	1001	1043
134-IVT31	7787	1018	991	1004	978	1018
IVT 32						
135-IVT32	1580	814	791	803	780	802
136-IVT32	8944	1039	1012	1025	998	1041
137-IVT32	1246	789	767	778	756	776
138-IVT32	5932	978	952	965	939	975
139-IVT32	8901	1038	1011	1025	997	1040
142-IVT32	1638	818	795	807	784	807
143-IVT32	1252	790	768	779	757	777
144-IVT32	1484	807	785	796	774	795
145-IVT32	1283	792	770	781	759	780
146-IVT32	1057	772	751	762	740	759
147-IVT32	1517	810	787	798	776	798
148-IVT32	1617	816	794	805	783	805
149-IVT32	1478	807	785	796	773	795
150-IVT32	1871	832	810	821	798	822

sample	Zr(ppm)	T(°C)12	T(°C)8	T(°C)10	T(°C)6	Tw(°C)
IVT 34						
174-IVT34	863	753	731	742	721	739
175-IVT34	1247	789	767	778	756	777
176-IVT34	8849	1037	1010	1024	997	1039
177-IVT34	7280	1007	981	994	968	1007
178-IVT34	8727	1035	1008	1022	994	1036
179-IVT34	8810	1037	1009	1023	996	1038
180-IVT34	1189	784	762	773	751	771
181-IVT34	9527	1049	1022	1035	1008	1051
182-IVT34	9847	1054	1027	1040	1013	1057
183-IVT34	1332	796	774	785	763	784
186-IVT34	1933	836	813	825	802	826
187-IVT34	2010	841	817	829	806	830
188-IVT34	1920	835	812	824	801	825
189-IVT34	1811	829	806	817	795	818
190-IVT34	733	737	716	727	706	723
IVT 33						
153-IVT33	9150	1043	1015	1029	1002	1044
154-IVT33	10079	1058	1030	1044	1017	1061
155-IVT33	2231	852	829	841	817	843
156-IVT33	8730	1035	1008	1022	995	1037
157-IVT33	9630	1051	1023	1037	1010	1053
158-IVT33	4878	950	925	938	912	946
159-IVT33	1014	768	747	758	736	755
160-IVT33	8845	1037	1010	1024	997	1039
161-IVT33	9710	1052	1025	1038	1011	1055
162-IVT33	11241	1076	1048	1062	1034	1080
165-IVT33	8244	1026	999	1013	986	1027
166-IVT33	10723	1068	1040	1054	1026	1072
167-IVT33	6120	982	956	969	943	980
168-IVT33	9590	1050	1023	1036	1009	1052
169-IVT33	8299	1027	1000	1014	987	1028
IVT 36						
010-IVT36	6027	980	954	967	941	978
011-IVT36	5563	969	943	956	930	965
012-IVT36	5721	973	947	960	934	970
013-IVT36	5390	964	939	951	926	961
014-IVT36	4220	931	906	919	894	926
018-IVT36	5143	958	932	945	919	954

Table 2 continued

sample	Zr(ppm)	T(°C)12	T(°C)8	T(°C)10	T(°C)6	T w(°C)
IVT 37						
029-IVT37	4413	937	912	924	899	932
030-IVT37	974	764	743	754	732	751
031-IVT37	1046	771	750	761	739	758
033-IVT37	3875	920	895	907	883	914
034-IVT37	648	726	705	716	695	711
035-IVT37	4297	933	908	921	896	928
036-IVT37	5711	972	946	959	934	969
037-IVT37	1670	820	797	809	786	809
038-IVT37	1951	837	814	826	803	827
041-IVT37	5344	963	937	950	925	960
042-IVT37	4747	947	921	934	909	942
043-IVT37	1648	819	796	807	785	807
044-IVT37	1281	792	770	781	759	779
045-IVT37	5854	976	950	963	937	973
046-IVT37	4468	939	913	926	901	934
047-IVT37	3369	902	878	890	865	895
048-IVT37	2796	879	855	867	843	871
IVT 38						
051-IVT38	4833	949	924	936	911	945
052-IVT38	972	764	743	753	732	751
053-IVT38	5230	960	934	947	922	956
054-IVT38	1457	805	783	794	772	793
055-IVT38	2866	882	858	870	846	874
056-IVT38	4267	932	907	920	895	927
057-IVT38	4304	934	909	921	896	928
058-IVT38	4206	931	906	918	893	925
059-IVT38	4748	947	921	934	909	942
060-IVT38	3573	909	885	897	873	903
063-IVT38	4352	935	910	923	898	930
064-IVT38	1142	780	758	769	747	767
065-IVT38	2170	849	826	838	814	839
066-IVT38	874	754	733	743	722	740

sample	Zr(ppm)	T(°C)12	T(°C)8	T(°C)10	T(°C)6
IVT 20					
039-IVT20	966	764	742	753	731
040-IVT20	2314	857	833	845	822
041-IVT20	1120	778	756	767	746
042-IVT20	1249	789	767	778	756
045-IVT20	1334	796	774	785	763
046-IVT20	1538	811	789	800	777
047-IVT20	991	766	745	755	734
048-IVT20	2007	840	817	829	806
049-IVT20	1627	817	795	806	783
IVT 40					
085-IVT40	1173	783	761	772	750
086-IVT40	1424	803	781	792	770
087-IVT40	1914	835	812	824	801
088-IVT40	1837	830	808	819	796
089-IVT40	3860	919	895	907	882
090-IVT40	996	767	745	756	734
091-IVT40	1853	831	809	820	797
092-IVT40	1329	796	774	785	763
093-IVT40	1467	806	784	795	773
094-IVT40	2792	879	855	867	843
098-IVT40	1248	789	767	778	756
099-IVT40	1313	794	772	783	761
100-IVT40	2033	842	819	830	807
IVT 42					
191-IVT42	2528	867	843	855	832
192-IVT42	4789	948	923	935	910
193-IVT42	4347	935	910	922	897
194-IVT42	1588	815	792	803	781
195-IVT42	2012	841	818	829	806
198-IVT42	3450	905	881	893	868
199-IVT42	1018	769	747	758	736
201-IVT42	2030	842	819	830	807
202-IVT42	1478	807	785	796	773
203-IVT42	2141	848	824	836	813
206-IVT42	1524	810	788	799	776
207-IVT42	1512	809	787	798	776

Table 3:Zr in Rutile temperature at different Pressure at a given Zr content

Zr=200				
P	TomEq1(°C)	TomEq2(°C)	TomEq3(°C)	T w(°C)
1	581	578	636	611
2	585	583	638	611
3	589	587	640	611
4	593	592	642	611
5	597	597	644	611
6	602	601	647	611
7	606	606	649	611
8	610	611	651	611
9	614	615	653	611
10	618	620	655	611
11	622	625	657	611
12	626	629	659	611
13	631	634	661	611
14	635	639	664	611
15	639	644	666	611
16	643	648	668	611
17	647	653	670	611
18	651	658	672	611
19	656	662	674	611
20	660	667	676	611
21	664	672	678	611
22	668	676	681	611
23	672	681	683	611
24	676	686	685	611
25	680	690	687	611
26	685	695	689	611
27	689	700	691	611
28	693	704	693	611
29	697	709	695	611
30	701	714	697	611

Zr=500				
P	TomEq1(°C)	TomEq2(°C)	TomEq3(°C)	Tw(°C)
1	652	647	713	687
2	657	652	716	687
3	661	657	718	687
4	666	663	720	687
5	670	668	723	687
6	675	673	725	687
7	679	678	727	687
8	684	683	729	687
9	688	688	732	687
10	693	693	734	687
11	697	698	736	687
12	702	703	739	687
13	706	708	741	687
14	711	713	743	687
15	715	718	746	687
16	720	723	748	687
17	724	728	750	687
18	729	733	752	687
19	733	738	755	687
20	738	743	757	687
21	742	748	759	687
22	747	753	762	687
23	751	759	764	687
24	756	764	766	687
25	760	769	769	687
26	765	774	771	687
27	769	779	773	687
28	774	784	775	687
29	778	789	778	687
30	783	794	780	687

Table 3 continued

Zr=1000				
P	TomEq1(°C)	TomEq2(°C)	TomEq3(°C)	Tw(°C)
1	715	708	781	753
2	719	713	784	753
3	724	718	786	753
4	729	724	789	753
5	734	729	791	753
6	739	735	793	753
7	743	740	796	753
8	748	745	798	753
9	753	751	801	753
10	758	756	803	753
11	763	762	806	753
12	767	767	808	753
13	772	772	811	753
14	777	778	813	753
15	782	783	816	753
16	787	788	818	753
17	791	794	821	753
18	796	799	823	753
19	801	805	825	753
20	806	810	828	753
21	811	815	830	753
22	815	821	833	753
23	820	826	835	753
24	825	832	838	753
25	830	837	840	753
26	835	842	843	753
27	840	848	845	753
28	844	853	848	753
29	849	858	850	753
30	854	864	853	753

Zr=1500				
P	TomEq1(°C)	TomEq2(°C)	TomEq3(°C)	Tw(°C)
1	755	747	825	797
2	760	752	828	797
3	765	758	831	797
4	770	764	833	797
5	775	769	836	797
6	780	775	838	797
7	785	780	841	797
8	790	786	843	797
9	795	792	846	797
10	800	797	848	797
11	805	803	851	797
12	810	808	854	797
13	815	814	856	797
14	820	820	859	797
15	825	825	861	797
16	830	831	864	797
17	835	836	866	797
18	840	842	869	797
19	845	848	872	797
20	850	853	874	797
21	855	859	877	797
22	860	864	879	797
23	865	870	882	797
24	870	876	884	797
25	875	881	887	797
26	880	887	889	797
27	885	892	892	797
28	890	898	895	797
29	895	904	897	797
30	900	909	900	797

Table 3 continued

Zr=2000				
P	TomEq1(°C)	TomEq2(°C)	TomEqn3(°C)	Tw(°C)
1	786	777	859	830
2	791	782	862	830
3	796	788	864	830
4	802	794	867	830
5	807	800	870	830
6	812	805	872	830
7	817	811	875	830
8	822	817	878	830
9	827	823	880	830
10	832	828	883	830
11	838	834	885	830
12	843	840	888	830
13	848	846	891	830
14	853	851	893	830
15	858	857	896	830
16	863	863	899	830
17	869	869	901	830
18	874	875	904	830
19	879	880	907	830
20	884	886	909	830
21	889	892	912	830
22	894	898	915	830
23	899	903	917	830
24	905	909	920	830
25	910	915	922	830
26	915	921	925	830
27	920	926	928	830
28	925	932	930	830
29	930	938	933	830
30	935	944	936	830

Zr=5000				
P	TomEq1(°C)	TomEq2(°C)	TomEq3(°C)	Tw(°C)
1	898	884	982	950
2	904	890	985	950
3	910	897	987	950
4	915	903	990	950
5	921	909	993	950
6	927	916	996	950
7	932	922	999	950
8	938	928	1002	950
9	944	935	1005	950
10	949	941	1008	950
11	955	947	1011	950
12	961	954	1014	950
13	967	960	1017	950
14	972	966	1020	950
15	978	973	1023	950
16	984	979	1026	950
17	989	986	1028	950
18	995	992	1031	950
19	1001	998	1034	950
20	1006	1005	1037	950
21	1012	1011	1040	950
22	1018	1017	1043	950
23	1024	1024	1046	950
24	1029	1030	1049	950
25	1035	1036	1052	950
26	1041	1043	1055	950
27	1046	1049	1058	950
28	1052	1055	1061	950
29	1058	1062	1064	950
30	1063	1068	1066	950

Table 4: Ti in Zircon temperature at different facies

Granulites			Low temp. eclogites			Eclogites		
Sample	Ti(ppm)	Tzr(°C)	Sample	Ti(ppm)	Tzr(°C)	Sample	Ti(ppm)	Tzr(°C)
HL01-1	6.3	702	QS45T-01	2.68	637	03LT1-1-1-1	3.4	654
	9	732	QS45T-02	6.38	703	03LT1-1-3-1	3.6	659
	3.9	665	QS45T-08	4.76	680	03LT1-1-8-1	4.8	680
	5.7	694	QS45T-10	3.58	658	03LT1-1-10-1	3.1	648
	5.1	685	QS45T-13	4.02	667	03LT1-1-17-1	4.4	674
	82.6	968	QS45T-19	3.37	654	03LT1-1-16-1	3.4	654
	6.2	701	QS45T-24	6.96	710	03LT1-1-18-1	2.2	623
	6.9	709	QS45T-25	4.25	671	03LT1-1-20-1	8.5	727
	7.7	719	QS45T-27	3.42	655	03LT1-1-22-1	4.7	679
	6.4	703	QS45T-30	4.42	674	03LT1-1-26-1	4	666
	4.7	679	QS45T-31	4.94	683	03LT1-1-24-1	26.9	836
	6.4	703	QS45T-32	3.63	659	06LT3-2-1-1	4.6	677
	8.9	731	QS45T-37	2.63	636	06LT3-2-3-1	3.4	654
	5.9	697	2Q27-1	19	801	06LT3-2-7-1	2.9	643
	5.8	695	2Q27-2	19.7	804	06LT3-2-6-1	63.1	934
	6.3	702	2Q27-3	16.2	785	06LT3-2-11-1	6.8	708
	7.9	721	15BJS-1-p	2.4	629	06LT3-2-15-1	13.9	771
	6.3	702	15BJS-2-p	5.1	685	06LT3-2-18-1	20.3	807
	4.6	677	15BJS-3-p	4.4	674	06LT3-2-19-1	97.8	991
	4.9	682	15BJS-4-p	10.5	745	06LT3-2-21-1	25	829
	16.3	786	15BJS-5	5.7	694	06LT3-2-20-1	16.2	785
	5.4	690	15BJS-6	3.18	649	07LT6-1-1-1	4.8	680
HL36-6	8.3	725	15BJS-7	3.52	657	07LT6-1-3-1	5.2	687
	9.1	733	15BJS-8	2.03	618	07LT6-1-5-1	3.1	648
	6.4	703	15BJS-9	10.9	749	07LT6-1-8-2	20.5	808
	8.6	728	15BJS-10	8.27	725	07LT6-1-9-1	3.3	652
	9.3	735	15BJS-11	10.6	746	07LT6-1-10-2	4	666
	14.4	774	15BJS-12	3.02	646	07LT6-1-17-1	3.3	652
	9.1	733	15BJS-13	6.15	700	07LT6-1-13-1	66.3	940
	8.4	726	HB121-13-6-r	11	749	07LT6-1-15-1	2.9	643
	8.4	726	HB121-13-8.1-r	5.2	687	07LT6-1-14-1	3.2	650
	7.6	717	HB121-13-8.2-r	4.9	682	07LT6-1-16-1	2.4	629
	11.1	750	HB121-13-9-c	2.4	629	LT10-2-1	6.9	709
	7.2	713	HB121-13-10.1-c 594	3.45	655	LT10-2-2	8.8	730
	9.6	737	HB121-13-10.2-c 1115	5.85	696	LT10-3-2	6.4	703
	8.2	724						

Table 5: Zr in Rutile temperature at different facies

Blueschist				
Sample	Zr(ppm)	Tw(°C)	T(°C)12	T(°C)18
SPH 991c				
	19	463	483	507
	29	485	506	530
	34	494	515	539
	40	504	524	549
	18	460	481	504
	23	473	493	517
	19	463	483	507
SPH 99 2	39	502	523	547
	35	496	516	541
	22	470	491	515
	22	470	491	515
	26	479	500	524
	27	482	502	526
SPH 99-3	38	501	521	546
	33	493	513	538
	38	501	521	546
	24	475	496	520
	20	465	486	510
	27	482	502	526
	15	450	471	494
	13	443	464	487
SPH 99 -5	31	489	510	534
	32	491	511	536
	31	489	510	534
	23	473	493	517
	43	508	528	553
	41	505	526	550
	38	501	521	546
	29	485	506	530
SPH 99-7	14	447	468	491
	23	473	493	517
	20	465	486	510
	28	484	504	528
	26	479	500	524
	18	460	481	504
SPH 99-8a	24	475	496	520
	44	510	530	555
	38	501	521	546
	37	499	520	544
SPH 99-8b	32	491	511	536
	14	447	468	491
	32	491	511	536
	30	487	508	532
	18	460	481	504
SPH 148a	26	479	500	524

Amphibolite			
Sample	Zr(ppm)	Tw(°C)	T(°C)9
Sample 1130	267	634	637
	268	634	637
	248	628	631
	254	630	633
	305	645	647
	313	647	649
	314	647	650
	287	640	643
	259	631	635
	299	643	646
	292	641	644
	302	644	647
	266	634	637
	286	639	642
	176	602	606
	237	624	628
	285	639	642
	274	636	639
	352	657	659
Sample 1184	323	649	652
	289	640	643
	428	673	675
	357	658	660
	378	663	664
	391	665	667
	420	672	673
Sample 1202	302	644	647
	250	629	632
	278	637	640
	274	636	639
Sample 1301	381	663	665
	176	602	606
	333	652	654
	301	644	646
	209	615	619
	340	654	656
	236	624	628
	399	667	669
Daixian samples	444	676	668
	415	671	662
	422	672	664
	363	659	651
	333	652	645
	363	659	651
	437	675	666
	392	666	658

Table 5 continued

Granulites

Sample	Zr(ppm)	Tw(°C)	T(°C)9.5
212-A-98	14.9	450	461
212-A-98	2880	875	868
212-A-98	1.05	336	349
212-A-98	1.7	354	367
212-A-98	403	668	672
212-A-98	148	589	596
212-A-98	1810	818	815
212-A-98	1878	822	819
212-A-98	1165	769	769
212-A-98	1589	803	801
212-A-98	1286	780	779
212-A-98	6.05	407	419
212-A-98	1304	781	780
212-A-98	1982	829	825
212-A-98	6.38	409	421
212-A-98	3174	887	879
212-A-98	1204	773	772
212-A-98	17.5	458	469
212-A-98	1225	775	774
212-A-98	1101	763	763
212-A-98	932	746	747
212-A-98	1836	820	816
212-A-98	1590	803	801
230-F-98	4.12	390	402
230-F-98	1236	776	774
230-F-98	3841	913	903
230-F-98	2.19	364	377
230-F-98	1405	789	788
230-F-98	998	753	753
230-F-98	1214	774	773
230-F-98	39.7	503	513
230-F-98	1015	755	755
230-F-98	15.8	453	464
230-F-98	40.3	504	514
230-F-98	25.7	479	489
230-F-98	111	569	577
230-F-98	1983	829	825
230-F-98	607	705	707
230-F-98	3299	892	884
230-F-98	894	742	743
230-F-98	351	656	661
230-F-98	132	581	588
230-F-98	12.3	440	452
230-F-98	700	718	720
230-F-98	2224	842	837
230-F-98	915	744	745

Eclogite

Sample	Zr(ppm)	Tw(°C)	T(°C)10	T(°C)15	T(°C)20	T(°C)27
H0906-1	27	482	494	514	534	550
H0906-2	28	484	496	516	536	552
H0906-16	31	489	502	522	542	558
H0906-4	36	498	510	530	551	568
H0906-10	37	499	511	532	552	569
H0906-11	29	485	498	518	538	554
H0906-12	42	507	519	539	560	578
H0906-17	32	491	503	524	544	560
H0906-18	30	487	500	520	540	556
H0906-20	38	501	513	534	554	571
H0906-21	36	498	510	530	551	568
H0906-22	39	502	514	535	556	573
H0907-4-1	19	463	475	495	515	529
H0907-4-5	34	494	507	527	547	564
H0907-4-6	21	468	481	500	520	535
H0907-4-7	29	485	498	518	538	554
H0907-14	27	482	494	514	534	550
H0907-4-3	29	485	498	518	538	554
H0907-4-4	33	493	505	525	546	562
H0907-5-1	44	510	521	542	563	581
H0907-5-2	39	502	514	535	556	573
H0907-5-3	36	498	510	530	551	568
H0907-5-4	44	510	521	542	563	581
H0907-3-1	18	460	473	492	512	526
H0907-3-2	25	477	490	510	530	545
H0907-3-3	24	475	488	508	527	543
H0907-6	60	528	540	561	582	601
H0907-9	39	502	514	535	556	573
H0907-10	50	517	529	550	571	589
H0907-11	37	499	511	532	552	569
H0907-16	18	460	473	492	512	526
H0907-17	31	489	502	522	542	558
H904-2-1	54	522	533	555	576	594
H904-2-3	49	516	528	549	570	588
H904-2-4	21	468	481	500	520	535
H904-2-11	17	457	470	489	509	523
H904-2-17	41	505	517	538	559	576
H903-2-9	329	651	658	683	707	734
H903-2	220	619	627	651	674	699
H903-2-10	325	650	657	682	706	733
H903-5-3	151	591	600	623	646	668
H903-3	216	617	626	649	673	698
H903-2-7	324	650	657	681	706	733
H903-6-2	221	619	628	651	675	699
H903-14	151	591	600	623	646	668
H903-2-8	325	650	657	682	706	733

Table 6:Comparison of Tzr vs Trt

IVT 01		IVT 20		03LT1-1		06LT3-2		07LT6-1	
Tzr(°C)	Trt(°C)	Tzr(°C)	Trt(°C)	Tzr(°C)	Trt(°C)	Tzr(°C)	Trt(°C)	Tzr(°C)	Trt(°C)
736	840	764	730	654	844	678	814	681	881
921	770	757	820	658	825	654	954	688	948
782	750	785	750	681	988	642	1028	647	987
742	770	771	760	647	915	954	838	818	959
1538	1010	727	770	674	913	711	852	651	883
801	1010	751	780	654	901	778	837	667	934
763	1040	764	740	621	788	817	826	651	847
		767	810	731	1018			961	860
		761	790	680	807			642	894
				667	857			649	833
				848	785			627	876